Daniel Filipe Félix Fernandes

Licenciado em Engenharia de Micro e Nanotecnologias

Transfer methods for arrays of nanostructures

Dissertação para obtenção do Grau de Mestre em
Engenharia de Micro e Nanotecnologias

Orientador: Doutor Pedro Miguel Cândido Barquinha,
Prof.º Auxiliar do DCM, FCT-UNL
Co-orientador: Doutora Rita Maria Mourão Salazar Branquinho,
Prof.º Auxiliar do DCM, FCT-UNL

Júri:

Presidente: Prof. Doutor Rodrigo Martins, Prof.º Catedrático do DCM, FCT-UNL
Arguente: Prof. Doutor Hugo Manuel Brito Águas, Prof.º Auxiliar do DCM, FCT-UNL
Vogal: Prof. Doutor Pedro Miguel Cândido Barquinha, Prof.º Auxiliar do DCM, FCT-UNL

FACULDADE DE CIÊNCIAS E TECNOLOGIA
UNIVERSIDADE NOVA DE LISBOA

Transfer methods for arrays of nanostructures

"*Boa sorte, cabeçinha fresca!*"

– Paulo Fernandes

ACKNOWLEDGEMENTS

Inicialmente, gostaria de agradecer aos professores Rodrigo Martins e Elvira Fortunato pela criação deste curso sobre a área fascinante da nanotecnologia e pela oportunidade de integrar o centro de investigação CENIMAT, cuja reputação é indiscutível a nível mundial.

Em segundo lugar, um enorme obrigado aos Professores Pedro Barquinha e Rita Branquinho pelo precioso acompanhamento dado ao longo destes meses de trabalho. Tive a oportunidade de integrar uma equipa muito profissional e coesa, que não só facilitou a minha integração no CENIMAT, como me ensinou a pensar e a trabalhar no campo de investigação científica. Sem os seus conselhos, o meu trabalho não seria o mesmo.

Deixo também o meu agradecimento à Ana Rovisco por todas as soluções e conselhos dados sobre os obstáculos que encontrei no decorrer do trabalho, provando ser vital para o desenrolar do mesmo. Obrigado por toda a paciência!

Obrigado a todos os meus colegas do CENIMAT que me acompanharam neste trabalho e por todos os óptimos momentos que me proporcionaram durante esta fase. Nunca esquecerei as jantaradas e, principalmente, os dias passados no laboratório com vocês. Um enorme obrigado pelo excelente ambiente que sempre imperou no decorrer desta etapa!

Olhando para trás, considero-me uma pessoa afortunada pelos amigos que me rodeiam e que me acompanharam durante toda esta fase. Entre todos os bons e maus momentos, vocês ensinaram-me a crescer em todos os sentidos e nunca conseguirei agradecer totalmente o vosso contributo para tal.

Ao pessoal da minha “terra”: Chico, Zedu, Viktor, Mário, Bola, Susana, Teka, PP, Timi ... ; Fizeram e fazem uma grande parte da minha vida. Todos os inúmeros momentos passados, sejam bons, sejam maus, nunca conseguirão ser descritos por meras palavras... Irei lembrar-me destes tempos para sempre.

Ao pessoal do Tico: Jaime, Pinto, Lima, Gabriel, Almeida, Carolina, Ana, Phelps, Mitra.. O grupo que me deu os momentos mais bonitos que tive na faculdade. Aulas fabulosas de Análise, muitas horas de volta das cartas e do snooker mas, principalmente, muitas e muitas horas acompanhado pelos melhores. Ainda revejo várias vezes o vídeo do “Pintainho”, que não precisa de introduções! Um grande, grande obrigado a vocês todos!

À malta do Núcleo (e maioritariamente de Materiais): Cardoso, Relvas, Infante, Esgrima, André, Loures, Duarte, Rodrigo, Dias. Obrigado pela vossa boa disposição em todos os momentos que passamos juntos. Farão sempre parte das pessoas mais marcantes e importantes com que me cruzei nesta faculdade!

Ao Ricardo, grande amigo desde os tempos escolares, que não precisa de introduções nenhumas. Sabes bem tudo o que passamos e vivemos durante esses anos e, apesar de estarmos em margens opostas, sei que quer passe uma semana, um mês, um ano ou mais, irei sempre ter a tua presença como garantida. Obrigado por todos os momentos e aventuras que tivemos e que venham mais!

À Patrícia e à Andreia, por todos os momentos que passamos juntos, a andar dum lado para o outro ou mesmo só sentados na Samadi. Foi uma excelente fase, que vou guardar com muito carinho. Espero que daqui para a frente nos consigamos encontrar com mais frequência!

Ao Diogo, Imo, Gordo e, mais recentemente, Cação. Rapidamente me senti acolhido por todos vocês. Rapidamente senti que estava no meu elemento com vocês. Acima de tudo, rapidamente me senti bem com vocês. Nunca me esquecerei das viagens a Ansião (para o ano há mais!) e de todos os momentos da mesma. N+G.

À minha namorada, Ana Lúcia. Este agradecimento é, sem sombra de dúvidas, dos mais difíceis de escrever. Nem sei por onde começar. Tu és, de longe, uma das melhores pessoas que já conheci na minha vida, que todos os dias me faz sorrir. Desde que te conheci que me contagias com a tua alegria, frontalidade e descontração. Fazes-me sentir progressivamente mais completo. Muito, muito, muito obrigado pela tua presença na minha vida e pela maneira como

abriste as portas da tua vida para mim. Nunca vou esquecer todos os momentos que já passamos e anseio cada vez mais pelo os que viram. Amo-te B!

Finalmente, aos meus pais e irmã. Se o agradecimento anterior já era difícil, este nem se fala. Não consigo, de todo, abranger tudo o que já passamos. Obrigado por todos os sacrifícios que fizeram para que eu e a minha irmã tivéssemos a melhor educação possível. Obrigado por toda a entrega. Obrigado por toda a paciência. Obrigado pelo infindável acompanhamento. Obrigado pelas inesquecíveis viagens de carro pela Europa inteira! Acima de tudo, muito, muito, muito obrigado pela maneira como me ensinaram a ser a melhor pessoa possível. Eu sou a pessoa que sou hoje, graças a vocês.

ABSTRACT

Nowadays, semiconductor and metallic nanostructure compounds can be synthesized through a wide variety of techniques. However, their implementation in devices typically requires the use of transfer methods, in order to take nanostructures into specific substrates' areas. The application of these methods remains challenging as they cannot fulfill several attributes namely low cost, suitability for a large variety of nanostructures and compatibility with large area and/or thermal-sensitive substrates.

This work focuses on the study of two transfer techniques aiming to surpass these limitations, NanoCombing Assembly (NCA) and Rubbing, showing their applicability to deposit on low-cost substrates, aligned and random nanostructure arrays, respectively. Despite being difficult to transfer aligned nanowire arrays with NCA, Rubbing shows good results when depositing random networks, allied with process straightforwardness, low cost and high substrate compatibility compared to other methods. Polydimethylsiloxane (PDMS) is used as a nanostructure transport layer and transfer tests proved to be efficient on flat and patterned substrates. However, the low nanostructure adhesion to substrate's surfaces limited the electrical characterization of transferred patterns. Nevertheless, Rubbing shows great promise for cost-effective and simple transferring of micro/nanopatterns into large area substrates, if further optimization of the nanostructure/substrate interface is realized.

Keywords: Transfer; Nanowires; Cost-effective; Scalability; Reproducibility

RESUMO

Hoje em dia, a síntese de vários compostos metálicos e semicondutores, constituintes de nanoestruturas, pode ser feita através de várias técnicas. De modo a possibilitar a sua integração em dispositivos, são necessários métodos de transferência para colocá-los em zonas específicas dos substratos. Porém, estes métodos revelam-se complicados pois a sua execução é apenas possível para uma pequena gama de nanoestruturas e substratos de reduzidas áreas, intolerantes a processos de elevada temperatura.

Este trabalho visa o estudo de duas técnicas de transferência, NanoCombing Assembly (NCA) e Rubbing, que poderão não só ultrapassar estas barreiras, como viabilizar a deposição de nanoestructuras alinhadas e desordenadas, respectivamente, em substratos de baixo custo. Apesar das adversidades encontradas na deposição de estruturas alinhadas através do NCA, a transferência de nanoestruturas desordenadas com o Rubbing originou bons resultados. Além disso, trata-se de um processo simples, barato e compatível com muitos substratos. Polidimetilsiloxano (PDMS) é usado como base de transporte para as nanoestruturas e, nos testes de transferências efectuados, revelou-se eficiente em substratos lisos e padronizados. No entanto, a baixa adesão das nanoestruturas ao substrato alvo, torna a sua caracterização eléctrica inviável. Não obstante, se a interface entre as estruturas e o substrato for optimizada, o método Rubbing revela grande potencial na transferência de micro/nanopadrões para substratos de grandes áreas, sem apresentar elevado custo e complexidade.

Palavras-Chave: Transferência; Nanofios; Baixo Custo; Escalabilidade; Reprodutibilidade

LIST OF ABBREVIATIONS

AAO – Anodic Aluminum Oxide
AFM – Atomic Force Microscopy
ALD – Atomic Layer Deposition
AR – Anchoring Region
BBF – Blown-Bubble Film
BLC – Bottom Left Corner
BRC – Bottom Right Corner
CA – Contact Angle
CoO – Cost of Operation
CR – Combing Region
CVD – Chemical Vapor Deposition
DRP – Differential Roll Printing
DUV – Deep Ultraviolet
EBL – Electron-Beam Lithography
EUV – Extreme Ultraviolet
FETs – Field-Effect Transistors
HB – Hard Bake
IC – Integrated Circuit
ID – Identification Number
μCP – Micro-Contact Printing
MBE – Molecular Beam Epitaxy
MWNTs – Multi-Walled Nanotubes
NCA – NanoCombing Assembly
NIL – NanoImprint Lithography
NPs – Nanoparticles
NTs – Nanotubes
NWD – Nanowire Density
NWs – Nanowires
OL – Optical Lithography
PDs – Photodiodes
PDMS – Polydimethylsiloxane
PEB – Post-Exposure Bake
PEN – Polyethylene Naphthalate
PR – Photoresist
PRT – Photoresist Thickness
RM – Replica Moulding
RT – Room Temperature
SL – Soft Lithography
SP – Sweeping Print
Std Dev – Standard Deviation
SWNTs – Single-Walled Nanotubes
TLC – Top Left Corner
TRC – Top Right Corner
VdW – Van der Walls
VLS – Vapor-Liquid-Solid
VPE – Vapor-Phase Epitaxy
VSS – Vapor-Solid-Solid
WW – Water Wedging

LIST OF SYMBOLS

P – Pressure
F – Force
A – Area

TABLE OF CONTENTS

LIST OF FIGURES

LIST OF TABLES

1. MOTIVATION AND OBJECTIVES

1.1 Motivation

In today's modern world, nanostructures are becoming a crucial part of almost every device due to the enormous evolution registered in the field over the last 70 years.[1] The assembly of nanostructures, structural architectures with at least one nanoscale dimension (~1-100nm), can be obtained by a series of top-down and bottom-up fabrication methods like OL (Optical Lithography) and ALD (Atomic Layer Deposition), respectively.[2,3] Figure 1.1 depicts the evolution of lithography and transistor costs throughout the years. Despite being able to produce high-quality micro/nanopatterns, the involved high manufacturing and operation costs, high compound specificity, low large-area substrates compatibility and necessity of complex systems urged the search of new alternatives to fabricate these structures.[4–7] Additionally, the number of transistors bought with a fixed price of $1 increases until certain point. From 2014 forward, the number of transistors starts to decrease mainly due to the fabrication processes' complexity and costs, reinforcing the need for other assembly alternatives.[8]

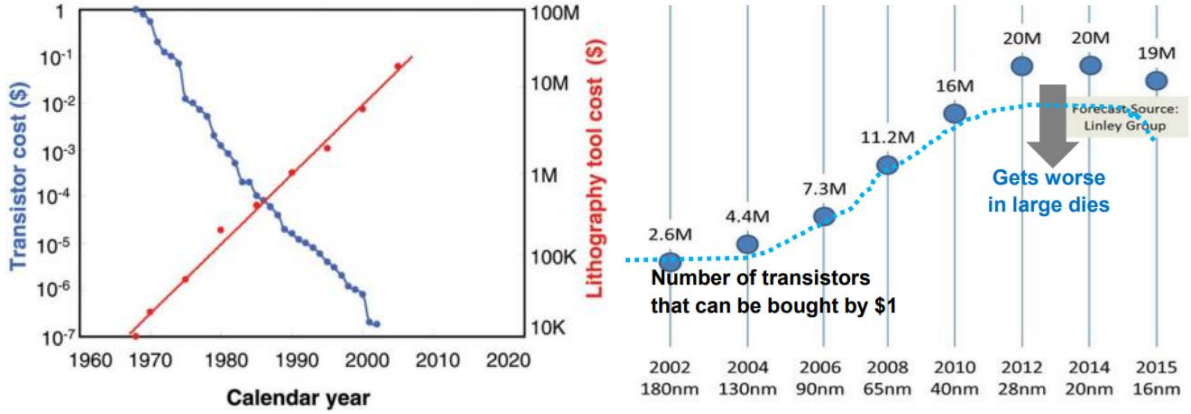

Figure 1.1 - Cost evolution of lithography processes throughout the years, related to the transistor costs also.[8,9]

Techniques based on SL (Soft Lithography), like μCP (micro-Contact Printing)[5,7] or RM (Replica Molding)[10,11], or NIL (NanoImprint Lithography)[12,13] are suitable competitors capable of producing nanostructures and also surpassing most of the mentioned challenges.

1.2 Objectives

This thesis objective resides on the study of nanostructures' transfer methods that are cheap, simple, scalable to large areas and compatible with a wide variety of substrates and compounds. Therefore, NCA (NanoCombing Assembly) and Rubbing methods were addressed aiming to transfer ordered and random NW (Nanowire) arrays, respectively. To fully assess NCA's capabilities, several parameters were studied as PR (Photoresist) layer thickness and morphology, transfer's speed and pressure and substrates' surface treatments. Seed layer synthesized ZnO (Zinc Oxide) NWs were used, being transferred to PR-patterned glass substrates. On the other hand, Solution-based synthesized Ni (Nickel) and ZTO (Zinc Tin Oxide) NWs were delivered, using flat and patterned PDMS (Polydimethylsiloxane), to PR-patterned glass, flat glass and flat PEN substrates, through Rubbing. Substrates' surface treatments, NW mass, PDMS patterning and water deposition were studied to optimize the Rubbing methodology.

2. INTRODUCTION

As the demand for smaller devices keeps increasing, fabrication techniques with higher resolution and aspect-ratio are needed to sustain such miniaturization. Due to the investment put on these processes, production of nanometric components milestone was achieved around the 2000s, as seen in Annex A, which have at least one nanoscale dimension (~1-100nm).[14,15] Widely recognized Top-Down methods such as OL (Optical Lithography) and EBL (Electron-Beam Lithography), are the most used by the semiconductor industry[5–7] aiming to produce these nanoscale components. However, as fabricated feature sizes tend to continuously decrease, the more complex Top-Down systems become. Inevitably, OL and EBL apparatus are becoming too expensive, as pictured in Figure 1, and other approaches need to be considered.[16–18] For instance, a EUV (Extreme Ultraviolet) OL system can cost ≈$50M whether a DUV (Deep Ultraviolet) OL is worth ≈$20M, neglecting its CoO (Cost of Operation) and maintenance, which can be quite expensive too.[10] Additionally, these techniques are not compatible with a broad variety of compounds and are not suitable for applications in large-area and thermal-sensitive substrates, thus making them unattractive for the semiconductor industry.

2.1 Bottom-Up Assembly: NWs

Thereby, Bottom-Up approaches were considered as they use nanoscale building blocks to assemble functional nanostructures, instead of standard Top-Down methodologies. NWs (Nanowires) are one-dimensional nanostructures that have been thoroughly studied due to their potential applications in electronic and photonic devices like FETs (Field-Effect Transistors)[19–21] and PDs (Photodiodes)[22–24], respectively. These structures are commonly composed of metallic and semiconductor materials and can be synthesized by various processes such as CVD (Chemical Vapor Deposition), Solution-Based and Metal Catalyst-Free Growth. NW growth by CVD has several variations like the VLS (Vapor-Liquid-Solid)[20,21,25–27] and VSS (Vapor-Solid-Solid)[22,28,29] mechanisms but, overall, these are methods that consist on the growth of NWs, mostly semiconductor NWs, using metal clusters/NPs (Nanoparticles) as catalysts. Metallic catalysts are deposited on top of a substrate, a generic semiconductor wafer for instance, and are heated inside a vacuum chamber. Annealing stages proceed, whose temperatures vary according to the type of CVD growth where the eutectic point of the substrate's material/catalyst group plays a major part in distinguishing all of its types[20,28,29], i.e. the temperature which Au/Si group melts if NW growth is desired on an Au-coated Si substrate, for example. When NW growth is conducted by a VLS process, applied heating must be above the eutectic point, whether by VSS's annealing temperatures should be below this point. Afterwards, a gas precursor containing the desired NW compound is introduced inside the chamber where its atoms will attach preferentially to the liquid metal catalyst. Through continuous insertion of the precursor, anisotropic growth will begin, attaining NWs in the end. Annexes B and C present VLS procedure and commonly synthesized NW compounds by VLS, respectively. Solution synthesis[30–33] is mostly used when metallic NWs are to be assembled and their production is based on chemical reactions with or without templates. The use of templates[22,34,35] such as porous AAO (Anodic Aluminum Oxide) usually helps in the wire's shaping but are not obligatory. This kind of synthesis usually requires some catalyst that will promote wire assembly in a solution containing the desired NW compound. Catalysts can be either suspended particles in the solutions or deposited on the growth substrate, acting as a seed layer[32,36]. Other NW synthesis methods are also reported that do not need metal catalysts such as MBE (Molecular Beam Epitaxy)[22,37] or VPE (Vapor-Phase Epitaxy)[38,39]. Generally, a gas containing the desired NW compounds is inserted in low- or even ultra-low-vacuum atmospheres and their atoms attach to the catalyst on the desired growth surface.

Nevertheless, these processes have some drawbacks regarding the annealing stages, synthesis duration, low-vacuum atmospheres and growth substrates' compatibility. Despite the high control witnessed in terms of grown NW's diameter, length and positioning, CVD and Epitaxy are pricey methods that involve high-temperature annealing stages[20,26,28] (500-1000 ºC), low-vacuum ambients (1.0×10^{-10} mbar [28]) and specific semiconductor substrates like Si wafers. Solution-based processes do not need such particular conditions and assemble a greater NWD (Nanowire Density), compared to CVD and Epitaxy procedures. However, these are lengthy methods (10-20 hours[32]) and grown NW's uniformity is harder to control. Additionally, if a seed layer is deposited on the substrate, synthesized NWs will grow all over the layer without any sort of

alignment or positioning. By that, if one can focus entirely on attaining the best NW synthesis possible, better approaches can be inspected towards obtaining the best NW arrangement, where Transfer methods can play a major role.

2.2 Transfer Methods: NWs

Along these lines, Transfer methods aim attention at the deposition of pre-grown nanostructures on desired substrates with high uniformity, feasibility and simplicity. Additionally, these methods ought to be cheap, compatible with large-area and/or thermal-sensitive substrates and with a wide variety of compounds. Intending to deliver NWs to a specific substrate, several transfer techniques were reported, in which DRP (Differential Roll Printing)[40], SP (Sweeping Print)[41], BBF (Blown-Bubble Film)[42], WW (Water Wedging)[43], NCA (NanoCombing Assembly)[44] and Rubbing[45] stood out from the rest, since most of the mentioned requirements were attained by each. These methods will be briefly described and their results shown in terms of transferred NWs alignment, NWD and other relevant features. Emphasis is done to the most promising ones, NCA and Rubbing.

DRP[40] is a process in which NWs are grown on a cylindric roller and are transferred to the desired substrate upon contact with it. This process is not specific to a certain NW compound or substrate material. The utilized NWs, of semiconductor compounds, are grown by VLS without any sort of positioning, aiming to transfer the highest NWD in the end. Accordingly, NW assembly regions are defined on the transfer substrate with a PR (Photoresist) layer through typical OL and are subsequently functionalized with a 0.1% w/v solution of poly-L-lysine. For transfer speeds under 20 mm/min and using a lubricant, Octane, to minimize contact friction, NWs detach from the roller by cause of VdW (Van der Walls) forces and are delivered to the assembly regions. >90% of transferred wires present alignment with ±5º deviation considering the printing direction, despite being randomly positioned on the assembly regions. PR layer can be removed afterwards with standard lift-off procedures leaving the aligned wires behind. This method can be performed at RT (Room Temperature) on small- and large-area rigid or flexible substrates and a transferred NWD of ≈6 NWs/μm was reported. However, standard lithography like OL is needed to predefine assembly regions and NWs need to be grown on cylindrical rollers every time the process is repeated. Annex D shows the used setup and some transfer results.

SP[41] methodology also relies on mechanical forces to transfer NWs to a certain substrate. NWs are grown by CVD on a rigid substrate and are mounted on a fixed stage, with the wires facing downwards, while the transfer substrate is mounted on a movable curved stage facing upwards, with a PDMS cushion between them. ZnO NWs and Kapton substrate were used in the reported trial. The movable plane is connected to an axis that enables circular movement, as shown in Annex E. Upon contact with the ZnO NWs, the Kapton substrate is moved counterclockwise and the wires are transferred due to the applied shear forces. This procedure is done at RT. Transfer results showed a NWD of ≈1.1×10^6 NW/cm^2 and a good degree of alignment, as seen in Annex E. However, NW alignment was not measured and they were randomly spread across the Kapton surface with inconsistent lengths.

BBF[42] transfer method is based on the contact and popping of a blown polymer bubble, with suspended NWs or NTs (Nanotubes), on a target substrate. Liquid polymer was produced by a mixture of THF and an epoxy resin, where the desired viscosity was attained after 20-30 hours by cause of the curing process. NWs and NTs are added in the THF before mixing the resin. The liquid polymer is then put inside a circular die and N_2 gas is blown through it, forming a bubble of liquid polymer with NWs/NTs suspended, as showed in Annex F. Due to the uniform bubble expansion, with the aid of a ring, along a defined direction, a certain degree of NW/NT alignment is attained. Contact of the polymer bubble with the transfer substrate will make it burst, transferring the NWs/NTs to the substrate's surface without jeopardizing their alignment. This technique was tested by delivering Si NWs, CdS NWs, SWNTs and MWNTs on Si wafers, plastics, curved surfaces and open frames, as pictured in Annex G, despite quantifying the alignment degree and NWs/NTs density on Si wafers only. Results show 80-90% Uniform defect-free NWs/NTs transferred films, high transfer reproducibility (bubble expansion rate 10-15 cm/min using 0.5-1.0 g of NW suspension), good degree of alignment (<±10º misalignment, regarding the expansion direction, on a 6 inch-wafer) and high NWs/NTs density (≈$4.0 \pm 0.5 \times 10^6$ NW/cm^2 using the polymer mix with 0.22 wt.% of suspended NWs/NTs). Some defects observed in the process related to the bubble/substrate interface were the air pocket's formation upon contact, preventing

transfer to the substrate, and the absence of some NWs/NTs from the bubble's outer surface, jeopardizing the yield of the transfer. Additionally, transferred nanostructures were randomly positioned despite the manifested alignment.

WW[43] is a transfer process based on the hydrophobic effect and has no mechanical steps like the ones witnessed in DRP and SP or long preparation times of NW's suspensions as in BBF. A wide variety of substrates, rigid or flexible, is compatible with the process and nanostructure's precise positioning is attained through the use a xyz-probe. To carry out the transfer, a hydrophilic glass slide containing a nanostructure on top of one of its sides is dip-coated with a hydrophobic polymer coating, whose constituent has great affinity with the nanostructure's material, thus housing it. As it is slowly dipped into water with a defined angle of incidence (30º or 150º considering the water meniscus), this hydrophobic coating will start to peel-off, bringing the nanostructure with it because of the high affinity between one another. When fully submerged, the hydrophobic coating containing the nanostructure will be suspended on the water. The desired substrate is put under water and, using the xyz-probe, transfer can be made by progressively removing the water. To finalize the process, dissolution of the hydrophobic coating is done, leaving the desired nanostructure on the target substrate. This method's steps and demonstration are depicted on Annexes H and I, respectively. Transfer can be attained at RT with high positioning precision on large-area substrates. However, water can be trapped between the nanostructure and target substrate when lowering its level, especially if a flexible substrate is used. The polymer coating also needs to be flexible enough to properly detach from the hydrophilic substrate upon dipping. This process was successfully tested by transferring graphene films onto semiconductor wafers and gold patterned films were also delivered but, this time, with a few problems regarding the hydrophobic coating's affinity with gold. More importantly and related to this thesis, NW transfer was not reported.

Most of the described transfer methods presented a great compatibility with rigid/flexible substrates, a wide range of NW compounds and were scalable to large-area surfaces but not all of them present good transfer uniformity and reproducibility. On the other hand, NCA's outcomes show a better NW alignment compared to the described methods and Rubbing enables the simplest and most cost-effective transfer of all, despite not guaranteeing any sort of nanostructure alignment in the end. Detailed description of these two processes is done below.

2.2.1 NanoCombing Assembly, NCA[44]

NCA is similar to DRP since a flat NW growth surface is used instead of a cylindrical roller to perform the transfer onto a PR-patterned substrate by friction. It aims to transfer highly ordered NW arrays with precise positioning. Reported results were obtained by transferring seed layer-grown Si NWs, with an average length of 30 µm, onto a PR-patterned substrate through direct contact between one another. Upon contact between both substrates, NWs' anchoring will occur on the exposed substrate areas. With constant pressure and speed, subsequent dragging of the seed layer substrate with determined direction will rip off NWs from the seed layer, transferring them. The final seed layer substrate movement originates friction that will induce the NW alignment, thus obtaining ordered arrays on top of the PR layer. Figure 2.1 depicts the process in its integrity.

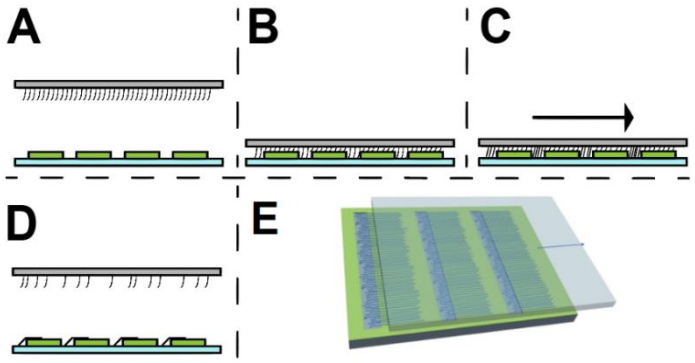

Figure 2.1 - NCA transfer process. (A) shows the NW growth substrate (gray) and the substrate (blue) with a PR-patterned layer (green), (B) the contact between both substrates, (C) the transfer direction and (D) the final outcome. (E) displays a 3D image of the process.

Yao *et al.*[44] stated that the need to have two very distinct, separate regions in the transfer substrate is imperative so anchoring and combing (or alignment) regions, AR and CR respectively, were carefully designed and optimized through OL. AR is a defined substrate's area that needs to have a strong interaction with the NWs so it's surface roughness and hydrophilicity need to be maximized. On the other hand, CR has to be exactly the opposite: a hydrophobic and planar surface, to minimize the interplay with the NWs. This difference will magnify the alignment forces since the NWs will be strongly anchored in AR and weakly adhered to CR's surface, making it very susceptible to the transfer's movement direction. AR is illustrated in Figure 2 as the exposed substrate areas in blue and CR as the PR-patterned layer in green.

Some important studies were conducted in this report, regarding AR/CR critical dimensions and NWD optimization. First, AR length needs to be at least 15 μm to maximize NWD, registered at 1,5 NW/μm. In this point, NWD saturates and stays put beyond it (Annex J and K(a)). This region is critical since it is here that the NWs will anchor one of their two edges, thus needing an adequate area to trap the highest number possible. If the AR is, by chance, smaller than 15 μm, so will be the transferred NWD. Secondly, CR layer cannot be thicker than 70 nm as NWD will decrease for greater sizes, caused by the lower probability of NW/AR contact. Annex K presents these relations. Additionally, transfer applied force and speed during the process were studied, showing a large independence of NWD whenever they stand between 2-6 N/cm^2 and 2-20 mm/min, respectively. Forcing the substrates too much against one another will likely damage the structures as well lower the NWD. Likewise, moving them too fast lessens the contact odds. Annex L exhibits these relations.

NCA transferred wires showed a higher degree of alignment compared to the previously stated, exhibiting 98.5% aligned NWs with ± 1º misalignment, thus showing very few crossing defects in the transferred arrays. Likewise, transfer speeds between 2-20 mm/min did not alter the final alignment, as shown in Annex L(a). More testing was done to assess the process' scalability and flexibility. Good alignment ratios were attained when transferring NWs to a 3x11 mm^2 area patterned with alternating 15x80 μm^2 sections. (Annex M) Also, bigger transferred wires were obtained when pre-grown NW were bigger but a large part of them is lost during the process. For instance, 30-μm long synthesized SiNWs end up 7-μm long in the end, owing to Friction (≈50%) and excessive trapped NW length in the AR (≈25%). Moreover, ≈140 μm-long NWs were successfully transferred with a 96% alignment within a variation of ± 1º. (Annex N) All of these experiments show the remarkable attributes that NCA has and shows the process' compatibility with bigger substrates and ability to transfer highly ordered NW arrays.

2.2.2 Rubbing[45]

Despite the mentioned output of NCA, it still relies on costly lithography to prepare substrates for transfer, for example. The Rubbing technique has a very similar procedure to a common SL method, as depicted in Figure 2.2, and the low-cost, simplicity and operation at RT are its most relevant attributes.

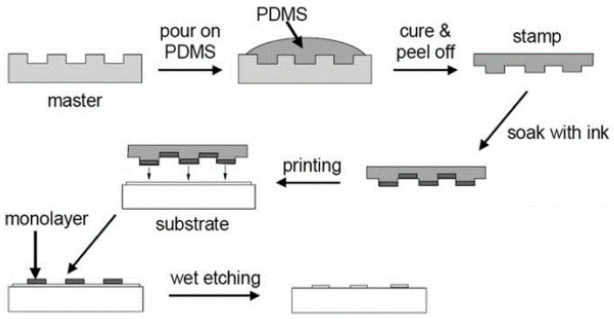

Figure 2.2 - Common SL methodology from the replica production until the end-product. This scheme is inspired in a reported SL process.[46]

Proposed by Biswas *et al.*[45], Rubbing was used to deposit a random layer of CuO NRs (Copper Oxide NanoRods) on top of vertically grown ZnO NRs, aspiring to obtain a p-CuO NRs/n-ZnO NRs heterojunction LED (light emission diode).

Initially, a GZO (Gallium-Zinc Oxide) coated glass substrate is patterned with a PR layer and ZnO NRs are grown vertically in the exposed GZO zones. To perform the transfer, a flat PDMS slab is rubbed with circular motion (Annex B, (a)) on top of a uniform CuO NR layer. As it is only desired to have the transferred NRs on top of ZnO rods, water is placed in the PR's cavities, precisely where ZnO NRs are. Pressing the PDMS attached-CuO layer on the patterned surface and freezing the water afterwards, will trap the rods on those specific zones. Subsequent PDMS peeling leaves the CuO NRs only on the desired locations and a final heating step is done to evaporate the water. In the end, a random compact CuO NR layer is deposited on top of ZnO NRs. Despite the initial lithography step, Rubbing is a technique independent of it since this beginning stage was only used to transfer in the desired areas. The whole process is depicted on Figure 2.3.

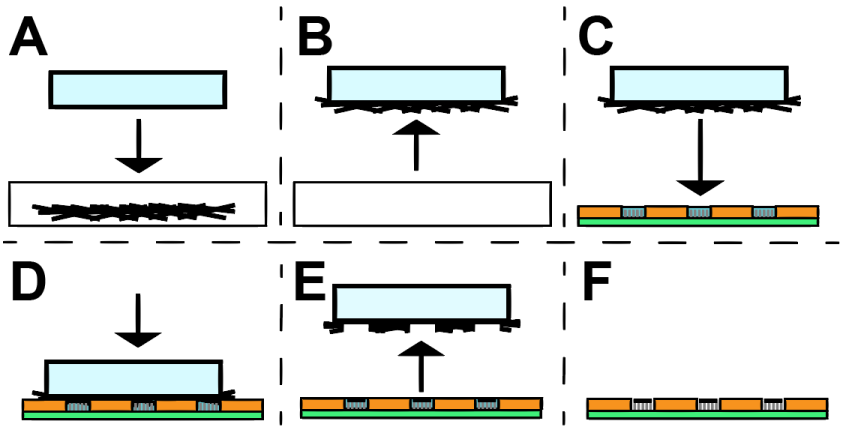

Figure 2.3 - Rubbing transfer method reported by Biswas *et al.*[45]. (A) represents the PDMS (light blue) rubbing step on CuO NRs and posterior removal, (B). Water droplets are delivered on the exposed substrate areas, (C), aiming to cover the exposed ZnO NRs (gray vertical lines) completely when the PDMS is pressed. (D) shows the contact step between both CuO NRs-coated PDMS and the patterned substrate. After freezing, the PDMS is peeled off, (E), leaving the CuO NRs (black horizontal lines) on top of the ZnO NRs (F). Glass substrate and PR patterns are illustrated in green and orange, respectively.

2.3 NW Compounds

Considering the chosen methods, NCA and Rubbing, one must choose NW compounds to perform the transfers with. ZnO is an oxide semiconductor material and was chosen since it is biodegradable, biocompatible[47] and suitable for a wide variety of applications such as optical biosensors[48] and solar cells[49]. ZnO NWs were used to perform transfer by NCA, thoroughly explained in the course of this work. As far as Rubbing is concerned, two different wires were chosen to realize the transfers: Ni and ZTO. Ni is a cheap metallic compound with ferromagnetic properties[50] that can be implemented in biosensors[51], for example. On the other hand, ZTO is an oxide semiconductor compound that presents high electron mobility. It is commonly used in TFT technology[52,53].

3. MATERIALS & METHODS

In order to successfully reproduce the previously described techniques, NCA and Rubbing, all of its elements need to be carefully studied and optimized. The following scheme in Figure 3.1 presents a summarized view of this work and all the addressed features for each method, from left to right.

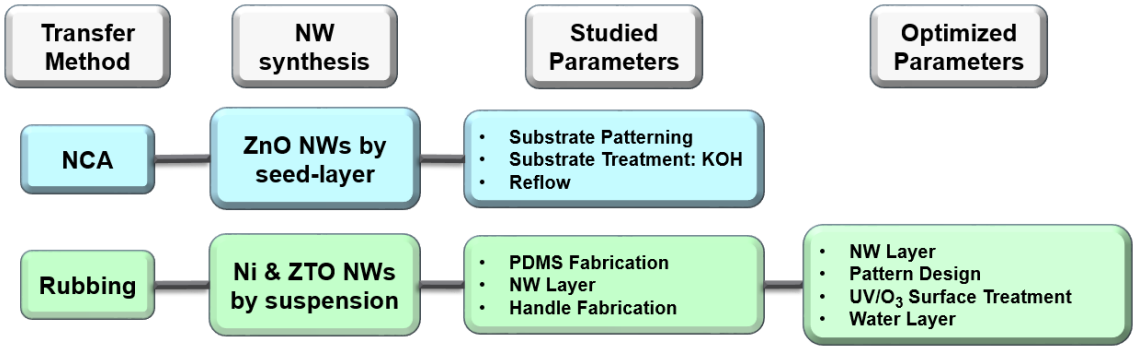

Figure 3.1 - Scheme for this work's addressed elements for each technique, from left to right.

3.1 NW synthesis

3.1.1 ZnO NWs by Seed Layer-Assisted Solution Method[54]

Initially, ZnO seed layer (~5 nm thick) was deposited on piranha cleaned glass substrates via sputtering. For the growth of nanowires, synthesis was carried out in a 100 mL autoclavable bottle containing aqueous solution mixture of hydrated zinc nitrate ($Zn(NO_3)_2{\cdot}6H_2O$) and hexamine (HMT, $C_6H_{12}N_4$). The seeded substrate, which was mounted on a glass slide, was kept within the solution, keeping the seeded face downward. The bottle was kept in an oven at 95° C for 6h. Afterwards, bottles were allowed to cool down to room temperature naturally and the substrates coated with white layer were washed thoroughly with DI water. Finally, the substrates were dried at room temperature. This synthesis was carried out by Dr. Soumen Maiti from CENIMAT.

3.1.2 Ni NWs[55] and ZTO NWs[56] by Solution Method

Ni NWs synthesis process is based on a solution method in which Ethylene Glycol is mixed with Nickel(II) Chloride ($NiCl_2{\cdot}6H_2O$) in a glass beaker. The solution is put for 10 min. under 120ºC heating. Later, Hydrazine Hydrate ($N_2H_4{\cdot}6H_2O$) was added to the mix and another heating step was done for 1 hour at 120ºC, finalizing the synthesis.[55] This synthesis was carried out by MSc Rodrigo Santos from CENIMAT.

ZTO NWs production is also based on a solution method, where 0.04M of Zinc Chloride ($ZnCl_2$), 0.02M of Tin(IV) Chloride ($SnCl_4{\cdot}5H_2O$), 0.24M of Sodium Hydroxide (NaOH), 7.5 mL of H_2O and 7.5mL of Ethylenediamine are mixed in an autoclave reactor. Posteriorly, the reactor is put in an oven at 200ºC for 24 hours, attaining the ZTO NWs. The resulting wires are washed several times with copious amount of H_2O and IPA, alternately. Finally, ZTO NWs are dried in a vacuum bell jar for 2 hours at 60ºC.[56] This synthesis was carried out by PhD Student Ana Rovisco from CENIMAT/CEMOP.

3.2 NanoCombing Assembly: Transfer of ZnO NWs

Aiming to transfer NWs through NCA[44], a similar setup was built, explained thoroughly below, and to achieve the highest yield possible, one needs to guarantee the best contact between NWs and ARs. Like so, the higher the number of NWs reaching the ARs surface, the more likely it is to get transferred NWs in the end. Along these lines, NWs were synthesized by a seed layer-assisted solution process and their contact with the ARs will be easier since they are perpendicular to these regions when contact between both transfer and NW growth substrates is done. Accordingly, patterned glass substrates were conceived by OL technology to properly delimit the ARs and CRs.

3.2.1 Substrate Preparation

PR thickness of 70 nm is needed to establish the distinct anchoring and combing regions[44]. AZ® ECI 3012 was chosen and is a positive resist recommended for DUV Lithography processes. Spin-coated films are 1.2 µm-thick at 4000 rpm but can vary from 1.0 to 2.2 µm with different spin-coating parameters. To obtain the desired thickness, dilution needed to be done and ≥99.5% PGMEA (Propylene Glycol Monomethyl Ether Acetate, Sigma-Aldrich®) was the adequate thinner. Different PR:Thinner volumetric ratios were used, from 1:3 to 1:5, to fully assess the resulting thicknesses. Dilution ratios were recommended by MicroChemicals® staff.

To deposit the PR, common 10x10 cm^2 glass substrates were cut into 3x3 cm^2 pieces. These were cleaned in ultrasonic baths in successive steps: 10 min. Acetone followed by 10 min IPA. Glass substrates were then rinsed with DI Water to remove IPA excess and dried with N_2 Drying Pistol. Then, substrates were put on a heating plate at 115ºC for a few seconds to ensure no water is on their surfaces.

Afterwards, film spin-coating was done with SUSS Microtech Spinner using a two-speed sequential deposition: 10-sec at 3000 rpm and 20-sec at 4000 rpm. Diluted PR volume applied for spin-coating was 1 mL. After this, a soft bake was done for 1:15 mins at 115ºC.

Sample exposure follows to pattern the PR layer. The mask used for this stage was an I3N mask with 700 µm-wide and 2.5 cm-long tracks with 700 µm-wide gaps between them. On one of their edges, microelectrode contacts were patterned. Exposure was done with a KARL SUSS UV MA6 aligner for 3.5 sec in Soft-Contact mode, in which the mask is gently pressed against the PR-coated glass substrate. PEB (Post-Exposure Bake) at 110ºC for 1 min. follows to ensure proper PR patterning.

PR Development was performed with consecutive Merck® AZ MIF 726 developer 30-sec bath and two DI Water 30-sec baths.

Finally, HB (Hard Bake) was done with different temperatures for 1 min, as it will be explained in the Results section, thus finishing the lithography process.

3.2.2 Transfer Setup

To reproduce identical NCA transfer, a setup was experimented using a Film Applicator BYK Gardner to move the seed layer substrate on top of PR-coated glass substrate at constant speed. Since constant pressure needed to be done, a weight was put on the back of the seed layer substrate so it would apply the pressure evenly. Two identical glass slides were attached to the glass substrate with PR surface faced upwards, creating a long path to perform the technique. Just before transfer trials were executed, 40 µL of Baysilone M-350 Lubricant were added next to the PR-coated glass, the same volume used in the report.

When using the film applicator, the fixed weight on the seed layer substrates back enabled the movement. The system's beam was programmed to move at minimum speed (50 mm/sec) and, upon touching the weight, it would slide the ZnO NW seed layer on the PR-coated glass substrate, just after passing by the Baysilone liquid volume. Figure 3.2 shows the devised setup:

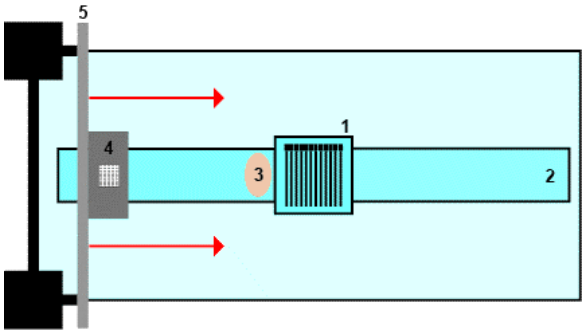

Figure 3.2 - NCA inspired transfer setup in which are pictured the patterned glass substrate (1), glass slide (right and left of the patterned substrate) (2), Baysilone Lubricant (3), Weight (4) and Film Applicator Beam (5). Note that the ZnO NWs substrate location is only representative since it was not positioned above the Weight, having the wires (black dots) in contact with the glass slide. The red arrows represent the beam's movement direction.

3.2.3 Substrate Treatment: KOH solution

Initially, glass substrates were immerged in a 1.5% wt. KOH (Potassium Hydroxide) solution to improve their hydrophilicity and later in less concentrated solutions to prevent harmful reactions with the PR tracks, as it will be explained in the Results section. To develop a 100mL 1.5% wt. solution, ≈1.7 grams of ≥90% pure KOH flakes (Sigma-Aldrich) were mixed with ≈98.3 mL of DI Water by stirring. Other solutions used throughout this work were 0.5% wt. and 0.25% wt. solutions. For the 100 mL 0,5% wt. solution, ≈0.5 grams of the same KOH reagent were mixed with ≈99.5 mL of DI Water and, similarly, ≈0.25 grams of KOH flakes were mixed in ≈99.75 mL to produce the 0.25% wt. solution. All 3 solutions were conserved in separate covered glass flasks.

3.2.4 Reflow Trials

Reflow tests were done to alter the PR tracks roughness and square-edged profiles. According to the datasheet, a deliberate hotter HB step would diminish the sharpness of PR profile edges, thus obtaining a rounded PR track, like shown in Figure 3.3:

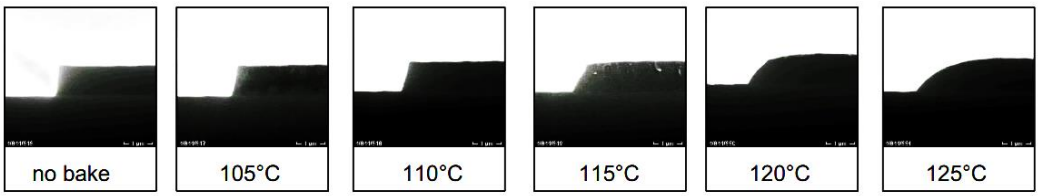

Figure 3.3 - Reflow tests and its effect on PR's profiles with increasing temperature. Taken from AZ® ECI 3012 datasheet.[57]

The main goal behind this experiment was to create softer tracks so that, upon combing, NWs would not break due to the sharp corners, attempting to improve the process' yield regarding combed NW length.

Likewise, different Development times were performed to check their influence on PR's profile.

3.2.5 Characterization

Fabricated Pattern PR tracks on glass were analyzed using Profilometer Sloan DEKTAK3, Profilometer Ambios XP200 and Asylum Research MFP3D Standalone AFM. AFM imaging was taken in Tapping Mode with Olympus AC160TS (K=26 N/m; Fø=300 kHz) and then processed with Gwyddion software.

Transfer results were inspected with Optical Olympus BX51 Microscope and processed through software Cell^A.

Substrate treatment was examined through contact angle measurements using Dataphysics OCA15plus equipment and software by Sessile-drop methodology. Water volume used for the measurements was 1 mL.

3.3 Rubbing Transfer of Ni and ZTO NWs

In order to perform transfer based on the Rubbing method, a uniform layer of NWs has to be attained, whose production is explained below. Solution-based NW synthesis was chosen since the wires are suspended in the end-product solution and can be stored in powdered form when removed from the solution. Also, the wires can be suspended in IPA without affecting their properties. Transfer based on Biswas *et al*.[45] uses PDMS as transfer layer for the NWs. These wires were dried and kept in powdered form to enable this use of PDMS, thoroughly explained below. Flat and Patterned PDMS were used to perform the transfers. Several substrates were tested as templates for the NW deposition: PR-coated Glass, whose fabrication is explained above, flat glass and flat PEN sheet.

3.3.1 PDMS Production

To synthesize PDMS, a mix of two reagents, Sylgard® 184 Silicone Elastomer and its Curing Agent, based on mass ratio, was done in a plastic cup. A 10:1 ratio (Elastomer:Curing Agent) was the most used in this work. For instance, if 20 grams of Silicone Elastomer were utilized, 2 grams

of the Curing Agent needed to be blend together to attain the ratio. Afterwards, the end-product needs to be mixed very well until it is full of bubbles. With a vacuum bell jar, sample was put under low-vacuum to remove all the bubbles, resulting in clear viscous PDMS. The mix was then poured in a plastic petri dish and was inserted in an oven for 1 hour at ≈65ºC to perform the curing step. If PDMS pouring creates more bubbles, they must be removed with the vacuum bell jar again, so that a uniform PDMS block is attained. Finally, the soft PDMS block was demolded from the petri dish and ready to be handled.

3.3.2 NW layer

In order to obtain a layer of synthesized NWs by solution-based methods, as explained above, one must disperse them in a liquid medium. For both compounds, Ni and ZTO, a small amount of them was mixed with a certain volume of IPA in a glass cylindrical vial. Through the use of an ultrasonic probe, the NWs were fully dispersed in IPA. This step lasts for at least 5 minutes to avoid NW aggregation. Afterwards, solution was put in petri dish and left to rest overnight to evaporate the IPA. In the end, a uniform layer of NWs was deposited on the petri dish's bottom, ready to be transferred.

3.3.3 Transfer Setup: Flat PDMS with Flat & Patterned Glass

PDMS integration caused some changes in the process. No longer using seed layer-grown NWs, small PDMS squares were cut from its production output. These were rubbed on top of the NW layer so that they could be deposited on the desired substrate.

To perform the transfer, DI water was used as a transport medium for the NWs. Some droplets of DI Water were put by hand on a chosen transfer area and the NW-covered PDMS surface was brought into conformal contact with the PR-coated glass/Flat glass where the water drops were positioned. Downward pressure is applied on the PDMS and excessive water amount is removed with filter paper. The whole group is then inserted in a freezer to solidify the water layer for at least 5 mins. It is extremely important to guarantee a proper water freezing so this step's time can be extended. Then, the PDMS layer was detached, leaving the NW on top of the glass substrate since the ice trapped them. Finally, the sample is put on a hot plate at ≈105ºC for a couple of seconds with the sole purpose of evaporating the water, leaving the NWs on the initially desired zone. This step is also very important and needs to be done quickly since the final patterned NW layer can be ruined if the water liquifies again.

3.3.4 Transfer Setup: Patterned PDMS and Flat Glass

Thereafter, transfer process using a patterned PDMS layer instead of patterned glass was executed. In order to pattern the PDMS, acrylic masters were done with a Laser System VLS3.50 Cutting Machine. Working with a 3-mm thick acrylic surface, desired patterns were designed with Adobe™ Illustrator software and carved in the acrylic surface. Patterns were then cut individually with the laser cutting machine.

Also, before PDMS patterning, acrylic masters need to go through silanization to ease PDMS peel-off. This stage was performed using a plastic vacuum chamber and PFOTS (trichloro (1H, 1H, 2H, 2H-perfluorooctyl) silane (97 %), Sigma-Aldrich). Inside the chamber, a plastic petri dish serves as a container for the silane compound, in which 2-3 droplets of it will be inserted. Acrylic masters are put in the chamber's dish and vacuum was done for 30 mins using a vacuum pump. Afterwards, air is admitted inside the chamber and acrylic masters are ready to use.

As mentioned in "PDMS production" section, after bubbles are removed using the vacuum bell jar, PDMS mix is poured in a plastic petri dish. To produce the master's replicas, pre-cured PDMS needs to be shed on top of the acrylic masters before its final curing stage. Two different paths were followed to produce the masters' replicas: Spin-Coating and Pouring. When spin-coating, PDMS is settled on top of the patterned acrylic masters and spinned at a maximum speed of 250 rpm for 1,5 minutes. The sample is taken to the oven at 85ºC for 1,5 minutes (curing time is significantly lower than the stated at "PDMS Production" section since spin-coated PDMS has a much lower thickness) and subsequently detached from the acrylic master. If a bigger PDMS replica thickness is desired, the acrylic master molds are put inside the petri dish with their pattern facing upwards. Then, PDMS is poured on top of it, almost filling the petri dish, as pictured in Figure 3.4. It is very important to check if the pattern is in contact with the dish's bottom to obtain a uniform PDMS thickness. The whole set is then put in an oven and demolded, just like it was

described in “PDMS Production” section. Ultimately, the soft PDMS block is cut by the boundaries of acrylic piece and detached from it, obtaining the patterned PDMS replica.

Figure 3.4 - Acrylic PDMS replica fabrication. This sequential process is done from left to right in which are pictured the PDMS layer (1), the Acrylic master (2) and the Petri dish (3). As described, PDMS block is demolded and then cut by the boundaries of the master. Patterned PDMS is posteriorly detached.

Using the Patterned PDMS chunks to transfer does not change the described process in the previous section. So, PDMS was put into contact with the NW layer and later in contact with the desired substrate, flat glass. Water was sandwiched between NW-coated PDMS surface and flat glass surface. Taking the whole system to freeze will trap the NWs inside the ice and upon detachment, these wires will remain on the glass’ surface. A final step of heating using the same temperature will evaporate the water, thus finishing the transfer.

3.3.5 Stamp Handle Fabrication

To pressure the PDMS stamp uniformly against the glass substrate, a handle was printed using a 3D Printer. Patterned PDMS was attached to the holder’s square surface using a double-sided tape, with its pattern facing downwards. Additionally, the handle’s weight will help improve the technique’s water freezing step, maintaining a certain pressure on the PDMS thus keeping a larger amount of NW immerged in the water layer. The handle’s 3D model is pictured on Figure 3.5:

Figure 3.5 - 3D model of the used stamp handle/holder. Square holder has a 4x4 cm^2 area whether the handle is ≈5cm tall.

3.3.6 Transfer Setup Optimization: NW & Water Layer and Pattern Design

Initially, when PDMS was implemented in the transfer process, the NWs mass was not weighted and a big chunk of wires was transferred but to obtain a proper uniform layer, mass needs to be considered so that transfer results can be compared accurately. Hence, a fixed mass of NWs was weighted then mixed with a certain volume of IPA and an ultrasonic probe was used to disperse the wires. The solution was poured into a square plastic box and left to rest overnight to evaporate the IPA, obtaining a more uniform NW layer.

The water layer is also very important for the success of this process. However, dropping a few droplets of water on top of the transfer substrate is an unprecise stage of the process. Water spin-coating was then considered aiming to obtain a uniform layer on top of the transfer substrate. Several tests were done and a recipe was obtained to deposit the water layer: 750 rpm for 5 seconds. The used spin-coater was a Spinner Laurell 2 (WS-650Mz-23NPP).

Additionally, after using KOH solutions to enhance substrates hydrophilicity, another treatment was tested: UV Ozone cleaning. KOH solution immersion achieved very good results within a short time but the KOH film uniformity was not consistent since, when dried, it left some spots on the substrate’s surface. UV Ozone treatment was then considered and Novascan PSD-UV10 was the device used to do so. In the case of glass, a 30-min UV-exposure is enough but PEN needs at least 1 hour to became highly hydrophilic.

3.3.7 Characterization

NW layer uniformity was inspected through the use of Optical Olympus BX51 Microscope and software Cell^A. Transfer results were also analyzed by the Optical Microscope and through SEM Hitachi TM 3030Plus Tabletop and SEM-FIB Zeiss Auriga CrossBeam Workstation.

UV Ozone treatment was checked using the same Contact Angle equipment and software from KOH treatment characterization.

4. RESULTS

4.1 NWs Synthesis

ZnO NWs were grown on a ZnO seed layer using the procedure explained in Materials & Methods Chapter. Measured NW lengths and diameters stood between 1.4-1.8 µm and 110-190 nm, respectively, as shown in Figure 4.1. Wires' production and evaluation were done by Dr. Soumen Maiti from CENIMAT.

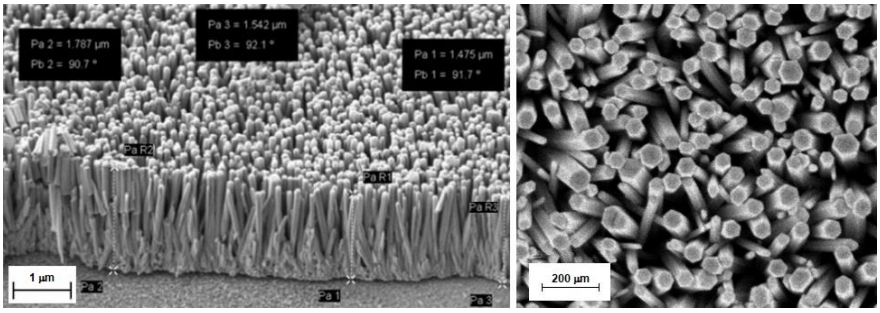

Figure 4.1 – SEM image of grown ZnO NWs by seed layer: lateral (Left) and top view (Right).

Ni NWs were grown by a solution-based procedure, explained in Materials & Methods Chapter. Synthesized wires had lengths of ≈60 µm and diameters of ≈1.9 µm on average, as represented in Figure 4.2. These NWs are formed through the agglomeration of Ni NPs, which are characterized by a rougher surface compared to the other used NWs.[58] Ni NWs were produced by MSc. Rodrigo Santos.

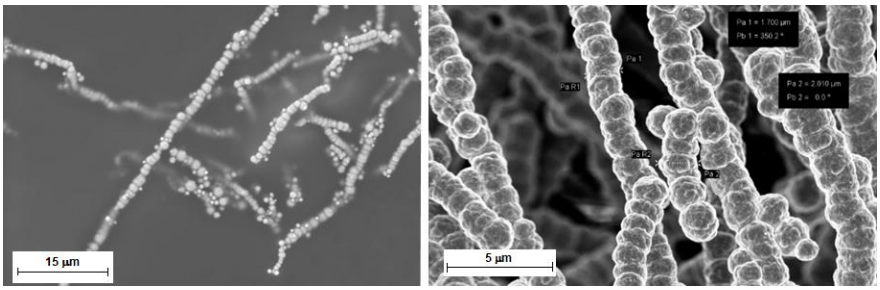

Figure 4.2 - SEM image of synthesized Ni NWs by a solution-based method.

ZTO NWs were also synthesized by a solution-based method, addressed in Materials & Methods Chapter. The wires were produced by PhD student Ana Rovisco and had lengths and diameters of 600 nm and 80 nm on average, respectively. Figure 4.3 shows the produced wires.

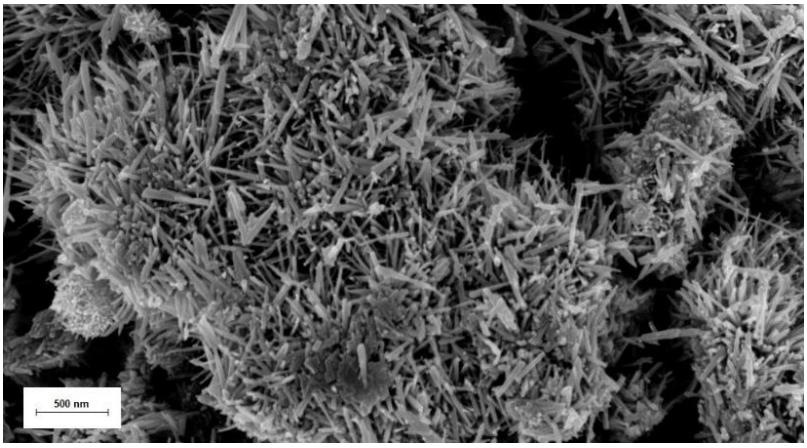

Figure 4.3 - SEM image of synthesized ZTO NWs by a solution-based method.

4.2 NanoCombing Assembly: Transfer of ZnO NW synthesized by seed-layer solution method

NCA procedure[44] implied the fabrication of patterned glass substrates in which AR and CR need to be well-defined so that similar NW transfer can be performed. PR coating and patterning on glass, identical to the assembled by Yao *et al.*[44], was done using a OL system. To do so and as explained in the Methods chapter, PR needed to be mixed with an adequate thinner using different volumetric ratios. PR dilution is crucial to the process since a proper PRT (PR Thickness) is required.

4.2.1 Substrate Fabrication: Photoresist Dilution

To obtain the necessary thickness of PR film on the glass, dilution tests were done using PGMEA as its thinner. Initially, 3 different PR dilution ratios were examined (PR:Thinner). PR layers were deposited on top of 3x3 cm^2 flat glass substrates but were not submitted to PEB and HB steps since in the end of the transfer process, after the NWs are combed, PR layer needs to be removed. PEB and HB stages aim to improve the desired pattern's resolution and toughness, respectively, but, as stated, PR removal finishes the process and it may prove to be very hard if these baking steps are done.[59] Figure 4.4 depict the final outcome of the OL procedure and used exposure mask.

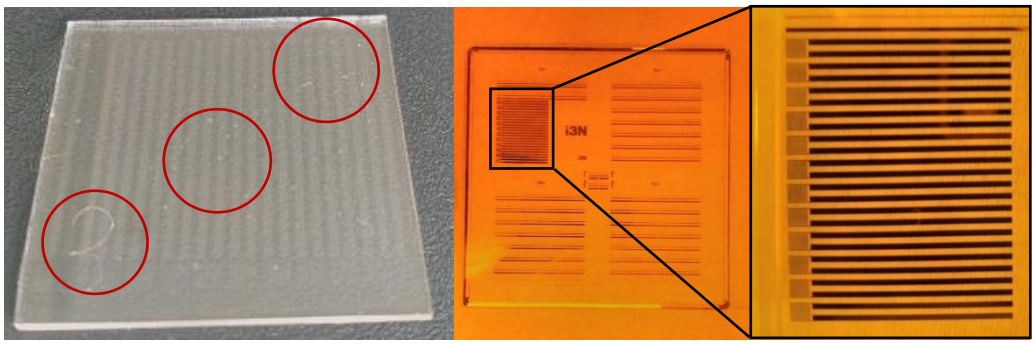

Figure 4.4 - 3x3 cm^2 PR-coated glass substrate (Left). The microelectrodes pattern area can be seen near the sample's ID number, 3. Red circles represent measurement locations, as explained below. Also, patterned Mask and section used in OL are pictured in the Center and Right, respectively.

PR thickness of these samples was evaluated through the use of Profilometer Sloan DEKTAK3, whose results are presented in Table 4.1. Height assessment was done in three different sample areas: Center, close to the sample's ID number and on the opposite of the ID number. In each spot, three measurements were done.

Table 4.1 - PR tracks heights of tested 1:3, 1:4 and 1:5 dilutions.

Dilutions (PR:Thinner)	Measurement Position	Thickness (nm)
1:3	Centered	77,8
	Close to ID	83,5
	Opposite to ID	84,5
1:4	Centered	47,4
	Close to ID	41,5
	Opposite to ID	48,4
1:5	Centered	35,9
	Close to ID	30,5
	Opposite to ID	48,9

Dilutions 1:3 and 1:4 ought to be the most promising towards obtaining 70 nm thickness. Like so, dilution ratios were tested and analyzed again using Profilometer Ambios XP200. This time however, the used dilutions were 1:3, 1:3.5 and 1:4, and were measured in five different sample

spots, three times: Centered, TLC (Top Left Corner), TRC (Top Right Corner), BLC (Bottom Left Corner) and BRC (Bottom Right Corner). Results are shown in Table 4.2.

Table 4.2 - PR tracks heights when 1:3, 1:3.5 and 1:4 dilutions were tested.

Dilutions (PR:Thinner)	Measurement Position	Thickness (nm)
1:3	Centered	107 ± 2
	TLC	105 ± 1
	TRC	106 ± 1
	BRC	103 ± 2
	BLC	104 ± 2
1:3,5	Centered	65 ± 5
	TLC	67 ± 8
	TRC	66 ± 7
	BRC	67 ± 7
	BLC	72 ± 6
1:4	Centered	67 ± 1
	TLC	69 ± 2
	TRC	64 ± 2
	BRC	66 ± 3
	BLC	72 ± 3

When comparing both tests, different thicknesses were obtained using the same dilutions, which is probably due to the age of the used PR, which was replaced later as mentioned in section 4.2.4. Nevertheless, the 1:4 dilution presents the best results of all dilutions. The 1:3.5 dilution also showed good results but with bigger PR height fluctuations, as we can see in Figure 4.5 when comparing 2 measurements taken from the exact same area.

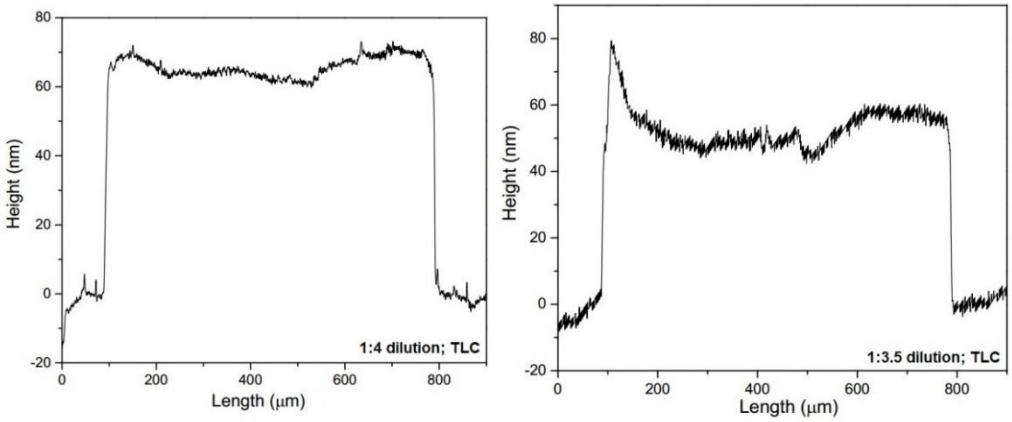

Figure 4.5 – Profilometer measurements and comparison of PR track profiles in the same area with different dilutions. Plot data was leveled.

In conclusion, the used PR, AZ® ECI 3012 is an adequate PR for the process and 1:4 dilution was the chosen one for the transfer process by cause of a more uniform thickness throughout the glass samples.

4.2.2 Transfer Setup

After the PR dilution, a similar NCA setup was designed to test the transfer methodology and infer the best improvements for it. The assembled system relies on the use of a film applicator and a weight, as explained in the Methods chapter. However, PR-coated substrate is not functionalized and the NWs' length is way smaller compared to the Si NWs used by Yao *et al.*[44], ≈30 µm (vs 1,4-1,8 µm). Figure 4.6 shows the whole assembly.

Figure 4.6 - Weight (Left), which was used to stick the seed layer substrate, and the setup (Right) to perform the transfer Note that, according to the sketch shown in Methods chapter, the weight is positioned on the glass tracks with the seed layer surface facing downwards, i.e. NWs are in contact with the glass track..

Promoting constant pressure, the weight was used to simulate the applied pressure reported by Yao *et al.*[44]. It is mentioned that, to avoid decreasing final NWD, a 2 to 6 N/cm^2 pressure is enough to promote reliable NW contact with the ARs. In order to do it, a weight was added to the system, as pictured in Figure 4.6. Several items were weighted and the one pictured above was the best among the rest, as proved below in Equation 4.1. This piece weighs ≈1.34 kg and the seed layer substrate has an area of 1,5x2 cm^2.

$$P = \frac{F}{A} \Leftrightarrow P = \frac{1{,}34\ kg}{3\ cm^2} \Leftrightarrow P = \frac{1{,}34\ kg * \frac{1N}{0{,}1kg}}{3\ cm^2} \Leftrightarrow P = \frac{13{,}4\ N}{3\ cm^2} \Leftrightarrow P = 4{,}47 \frac{N}{cm^2} = 4{,}47 \times 10^4\ Pa$$

(Equation 4.1)

Hence, this weight is acceptable to apply the needed pressure between 2 to 6 N/cm^2. Likewise, its shape was perfect for the process since it is similar to a square prism and did not touch anything else besides the seed layer substrate's back, when settled on the glass slides.

Evenly important, transfer speed was also checked but it was very different from reported. Yao *et al.*[44] stated that, to maximize NWD, transfer velocity should be within the range of 2-20 mm/minute and, in NCA, a 5 mm/minute speed was used. The film applicator moves its beam at a minimum speed of 50 mm/second, or 3000 mm/minute, an unquestionably enormous contrast. Unfortunately, this proved to be very challenging. Additionally, the lack of surface functionalization and long seed-layer grown NWs made further testing unreasonable.

Transfer results can be seen in Figure 4.7, in which the same lubricant volume reported was used, 40 µL. These proved to be a failure since no wires were transferred and the PR tracks were scratched and sometimes ripped off the glass substrate. The main reasons behind these results could revolve around the used weight, the transfer speed and the used NWs length.

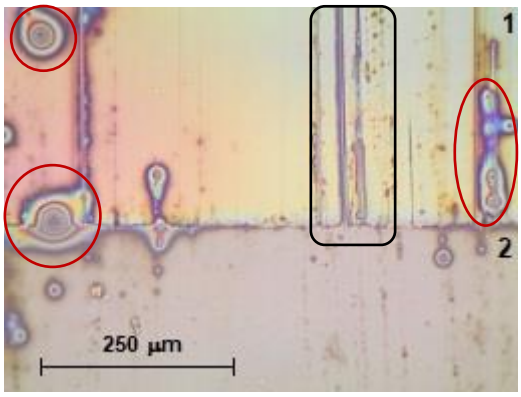

Figure 4.7 – Optical Microscope image of obtained transfer results from the initial NCA setup. PR tracks (1) show mechanically-induced scratching (black rounded square), most likely caused by the weight sliding. Lubricant contamination is also evident, highlighted through the red circles. (2) depicts the glass substrate's surface.

4.2.3 Substrate Treatment: KOH solution

After the unsatisfactory results of the assembled system, glass surface treatment was considered to promote a better NW adhesion to the ARs. Initially, CA (Contact Angle) analysis was done to flat glass and PR-coated glass substrates using the Dataphysics OCA15plus equipment (Annex O). The PR-coated glass surface was not patterned to ensure a proper assessment so one half of the sample is coated with PR and the other is not. Table 4.3 and Figure 4.8 exhibit the CA results for Flat and PR-coated Glass.

Table 4.3 - CA results of the flat and PR-coated glass substrates.

	Flat Glass CA		PR-coated Glass CA	
Drop#	Left (˚)	Right (˚)	Left (˚)	Right (˚)
1	53.0	53.0	74.4	74.6
2	56.0	56.0	74.9	74.8
3	49.9	49.6	75.4	75.3
4	48.0	48.1	75.8	75.7
5	52.1	52.2	77.7	77.6
6	53.3	54.0	77.8	78
Mean (˚)	52.0		76.6	
Std Dev (˚)	2.8		1.4	

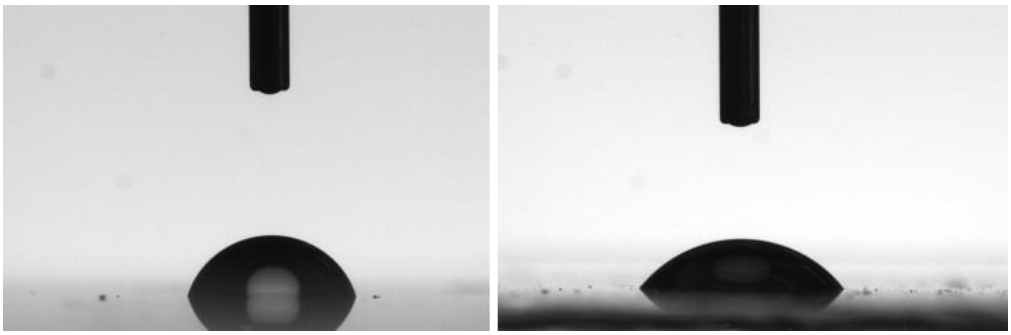

Figure 4.8 – CA measurements of 1 mL water drop on top of the PR-coated (Left) and Flat Glass (Right) surfaces.

Since it is of best interest to have a highly hydrophilic glass surface (AR) and a highly hydrophobic PR coating (CR), suggested KOH treatment by Yao *et al.*[44] was considered: a 50 second bath in a 1,5% wt. KOH solution. Hence, two experiments were done to evaluate the influence of the KOH treatment on glass and PR.

First off, a 3x3 cm^2 glass was coated with PR in one half whether on the other half was done nothing, as done above. PR coating was produced according to section “Substrate Fabrication: PR Dilution”. The sample was then immersed in 1,5% wt. KOH solution for 50 seconds and analyzed through CA measurements. Figure 4.9 shows the outcome of this test.

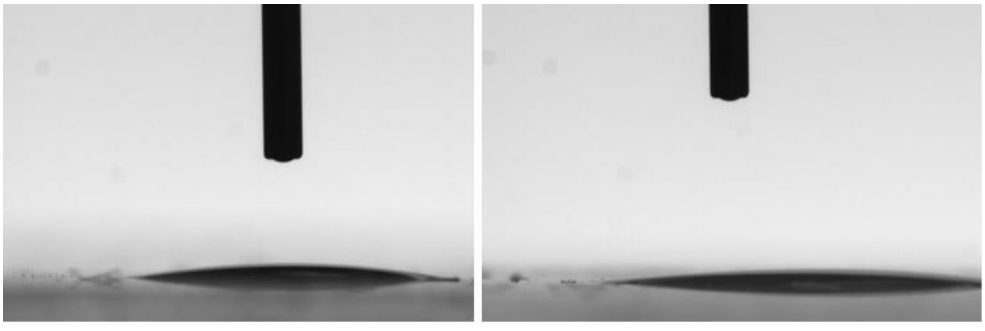

Figure 4.9 - CA evaluation of both surfaces when submitted to the KOH solution in the end. Flat Glass is on the left whether the PR surface on the right.

Treatment worked extremely well with the glass half, making its surface highly hydrophilic. However, the PR-coated half also became extremely hydrophilic, which should be as hydrophobic as possible. To better assess KOH influence on the layered substrate, this treatment was done before depositing the PR and was submitted to the same CA analysis in the end. Figure 4.10 and Table 4.4 exhibit the CA results for the flat glass half and the PR-coated half.

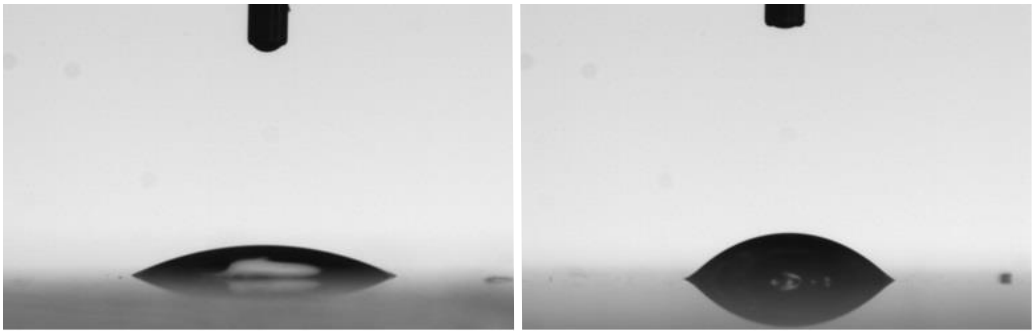

Figure 4.10 - CA measurements of 1 mL water drop on top of the non-coated (Left) and PR-coated (Right) glass surface. KOH was applied before the PR tracks.

Table 4.4 - CA results for both halves to assess the influence of the KOH coating on PR tracks, when applied first.

	Flat Glass Half CA		**PR-coated Glass Half CA**	
Drop#	Left (˚)	Right (˚)	Left (˚)	Right (˚)
1	20.9	24.6	45.0	45.0
2	25.6	24.4	43.5	43.5
3	26.3	26.6	46.5	45.6
4	25.8	23.1	29.7	29.7
5	28.2	27.7	36.2	23.3
Mean (˚)	25.3		38.8	
Std Dev (˚)	2.3		8.6	

Some changes were verified when the KOH treatment was done before substrate PR coating. As shown in Figure 4.10, there is a bigger difference in terms of hydrophilicity compared to the one registered in Figure 4.9. However, CA analysis on the PR-coated half displayed some measurements with very different angle values for the same drop as shown, for instance, on Drop #5 in Table 4.4. Likewise, in comparison with the registered values on the other presented CA tables, calculated Std Dev (Standard Deviation) of the coated half is almost four times bigger, which could be indicative of an inconsistent layer.

PR's properties were studied and the reason behind the odd results of CA analysis on the PR layer is the concentration of the KOH solution. Exposed AZ® ECI 3000 series PRs, in which AZ® ECI 3012 is included, tend to dissolve when submitted to ≥0.5% wt. KOH solutions. Therefore, other KOH solutions were synthesized, 0.5% wt. and 0.25% wt., and were tested on some flat glass substrates. Sample immersion time was established at 10 and 20 seconds per solution concentration. Results are exhibited on Table 4.5 and Figure 4.11.

Table 4.5 - CA values for different KOH concentrations and sample immersion times.

	10 second Immersion		**20 second Immersion**	
	0.5% wt. KOH	**0.25% wt. KOH**	**0.5% wt. KOH**	**0.25% wt. KOH**
Results	18.9˚ ± 1,8˚	20.5˚ ± 1,3˚	9.9˚ ± 1.4˚	9.9˚ ± 2.2˚

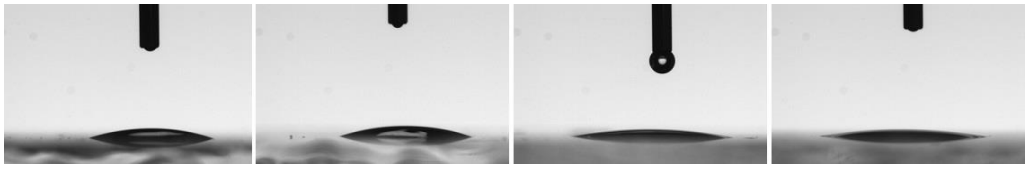

Figure 4.11 - CA measurements of 1 mL water drop on top of non-coated glass surfaces. The different KOH tests are ordered as in Table 4.5, i.e. 10 second immersion on 0.5% wt., 10 second immersion on 0.25% wt., 20 second immersion on 0.5% wt. and 20 second immersion on 0.25% wt., from left to right.

Table 4.5 shows that a longer sample immersion is beneficial to the glass surface and, in this case, both concentrations present identical CA values. However, considering the limit stated above regarding PR dissolution in >0.5% wt. KOH solutions, the chosen treatment was the 20 second immersion in 0.25% wt. KOH solution.

4.2.4 Reflow Trials

Hoping to work around the differences between the assembled setup and the reported one, another substrate treatment was considered to ease NW transfer and subsequent combing: PR Reflow. This approach was not done by Yao *et al*.[44] and, as seen in Figure 3.3 of the Chapter Materials and Methods, it aims to intentionally round the PR track's edges so that transferred NWs have a lower probability of breakage upon combing. Figure 4.12 establishes a comparison between both profiles.

Figure 4.12 - Comparison between normal PR track profile (Left) and after Reflow treatment (Right). Note that (1) is the glass substrate and (2) the PR layer.

Before inspecting this approach, replacement of the stored PR batch implied new dilutions tests to see if the chosen ratio was still adequate. Exactly the same procedures were done as in section "Substrate Fabrication: PR Dilution". Also, these samples were submitted to KOH treatment and to different developer bath times, 10, 20 and 30 seconds, to study its influence on PR track's heights. Table 4.6 displays the measured PR track's heights using the Ambios XP200 Profilometer.

Table 4.6 - PR tracks heights for tested 1:2 to 1:4 dilutions

Dilutions (PR:Thinner)	Measurement Position	Thickness_10s Development (nm)	Thickness_20s Development (nm)	Thickness_30s Development (nm)
1:2	Centered	115	104	109
	Close to ID	113	107	104
	Opposite to ID	109	116	102
1:2,5	Centered	97	88	85
	Close to ID	94	91	87
	Opposite to ID	103	98	91
1:3	Centered	69	64	69
	Close to ID	68	77	72
	Opposite to ID	67	79	74
1:3,5	Centered	59	44	47
	Close to ID	63	52	45
	Opposite to ID	69	46	46
1:4 (Previously Chosen)	Centered	52	47	41
	Close to ID	44	50	43
	Opposite to ID	57	48	38

Development time variation does not alter significantly the PR track's heights and aspect ratio but the longest bath time was chosen, a 30 second bath. Additionally, a new dilution ratio was chosen, 1:3 when the previous was of 1:4, which was implemented from here on.

To test the Reflow approach, HB stage temperature needs to be varied. Prepared substrates were initially KOH-treated and followed the same OL procedure but with a new PEB step, done for 60 seconds at 110ºC. This step was added to enhance the PR layer's resolution. Tested HB temperatures were identical to the presented range on PR's datasheet and also applied for 60 seconds. Figure 4.13 exhibits the PR track's profile measurements through the Ambios XP200 Profilometer.

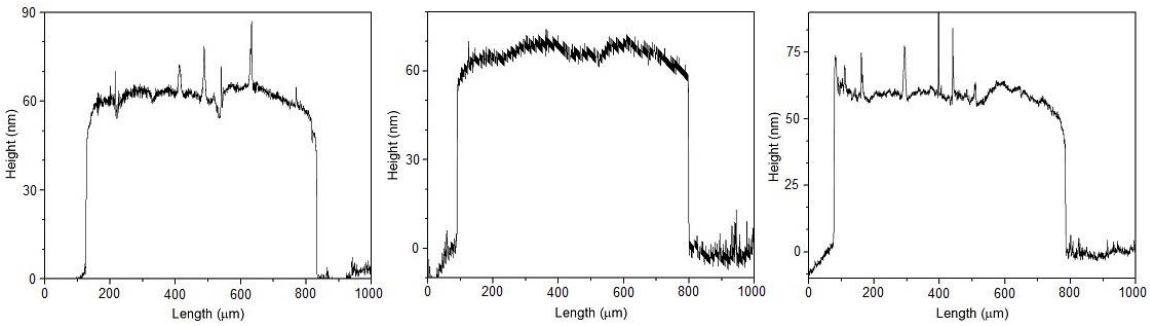

Figure 4.13 – Profilometer measurements of a PR track profile when a HB step of 110ºC, 120ºC and 130ºC is applied, from left to right.

Profile inspection on the tested temperatures shows that track rounding does not happen as prominently as seen in the PR's datasheet. After discussion with MicroChemicals® staff, it was decided to push these tests further, applying hotter and considerably longer HB steps. Thus, 5 minute-long 140ºC and 150ºC HB steps where done. Figure 4.14 shows the outcome of these trials.

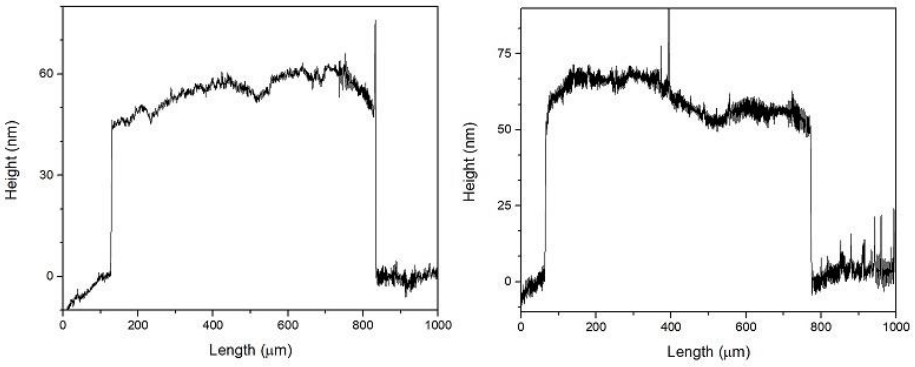

Figure 4.14 - Profilometer measurements of a PR track profile when submitted to a harsher HB stage of 140ºC and 150ºC, from left to right.

Even after these tests, Reflow was not witnessed on the patterned PR tracks. Hence, a more profound morphological characterization was done through AFM using Tapping Mode, as described in Chapter Methods. Figure 4.15 shows the results of 125ºC and 150ºC HB steps.

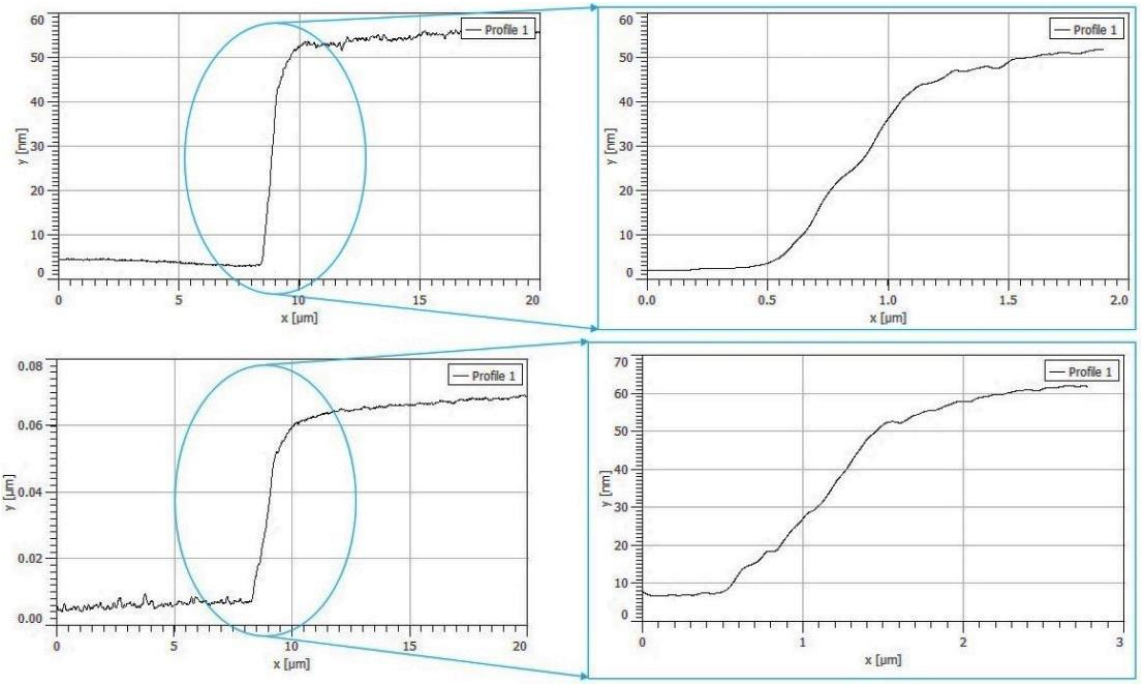

Figure 4.15 – AFM analysis and comparison of PR track profiles when exposed to HB 125ºC (Top) and HB 150ºC (Bottom) steps.

AFM investigation showed that Reflow actually happened, contrary to previous conclusions taken from the Profilometer measurements. The printed PR tracks are 700 µm-wide using the described OL conditions but when HB temperature is increased, a 2-4 µm enlargement happens, which is barely noticeable considering track's dimensions. After a brief discussion with MicroChemicals® staff it was concluded that the reduced PR volume per track is most likely the leading cause behind the less evident Reflow. Considering the chosen PR dilution ratio and height per deposited track, it is unreasonable to compare the demonstrated effect in the datasheet with the obtained diluted PR profiles. Also, as shown in Figure 3.3 on Chapter Methods, HB temperature increased impact on PR tracks was exhibited but it is related to the application of undiluted PR. Additionally, deposited patterns would be much thicker compared to the studied in this work if identical PR deposition conditions were to be used. Taking all these elements into account, one can state that Reflow effect happened but PR tracks did not have enough volume to manifest evident deformation as seen in Figure 3.3.

4.2.5 Limitations for applicability of NCA

Despite having the desired RT on printed PR patterns and a highly hydrophilic AR surface, other crucial parameters needed to be improved so that comparison with the original NCA setup can be done. Considering the conditions reported by Yao *et al*.[44], used film applicator's transfer speed is substantially faster, the seed layer-grown NWs are much smaller and the reflow treatment did not change substantially the PR track's profiles. Additionally, a OL exposure mask that could pattern the PR layer with identical dimensions could make the production of similar AR and CR easier. Like so, NCA's reproduction was unreliable and further testing was discarded.

4.3 Rubbing transfer of Ni and ZTO NW synthesized by solution method

Having in mind the limitations of the current NCA implementation explained in the previous section, other approaches were investigated and a PDMS rubbing technique reported by Biswas *et al*.[45] offered a simple and cheaper process that could possibly be merged with NCA or, if not, follow another path.

Biswas *et al*.[45] reported the transfer of random NW arrays with a flat PDMS layer using only water and a low temperature step. The process is quite simple, as elucidated in Chapter Methods, and

does not rely on OL processes to execute NW transfer. Hence, bearing all the specified flaws of previous setups in mind, the integration of this soft element was done.

4.3.1 First Trials

To fully assess this transfer method's key factors, a simple trial was done using a flat PDMS square, as a transfer layer, a flat glass substrate and Ni NWs. PDMS was produced with a 10:1 ratio, cut into squares using a one-sided straight blade and cleaned with IPA. The glass substrate was cleaned and the NWs settled as described in Chapter Methods. This experiment was aided by the report's author, Pranab Biswas, a Postdoc Researcher at CEMOP. Figure 4.16 shows the settled NWs and the transfer's product, from left to right.

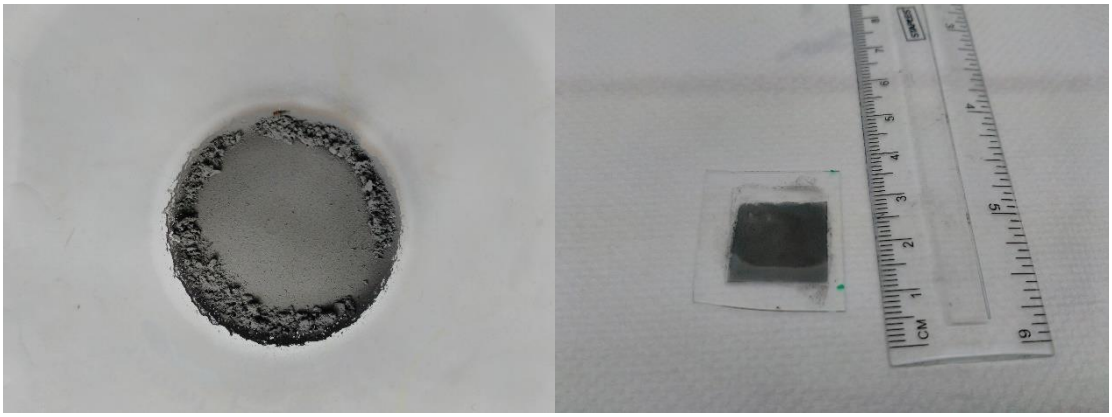

Figure 4.16 - First rubbing transfer trial using PDMS as a transfer layer (Left) and Ni NWs (Right).

This proved to be successful as seen in Figure 4.16 (Right) and was of moderately easy operation. However, some factors need to be taken into account to perform the best transfer possible. PDMS's straight cutting is essential to maintain side linearity and the NWs should be transferred through PDMS's top surface, i.e. the surface that is not in contact with the plastic petri dish during its production. Also, the settled NWs should form a uniform film, unlike what is shown in Figure 4.16 (Left), so that upon contact with the PDMS, a uniform NW layer can be transferred.

Some other trials were done to evaluate the reproducibility of this methodology using the same NWs and PDMS ratio and shape. Figure 4.17 shows the results.

Figure 4.17 - Repetition of the first trial of rubbing transfer using PDMS as a transfer layer and Ni NWs, showing process reproducibility.

Accordingly, reproducibility was barely attained. None of the 3 experiments resulted in a clean transfer, compared to Figure 4.16, presenting a significant number of gaps in the transferred area. These defects were most likely a consequence of excessive water volume and/or ineffective water freezing, the remaining key factors contributing to the success of the transfer method. One needs to be certain that the water transport layer is properly frozen before detaching the PDMS and this

depends on the water volume used to transfer and the time spent in the freezer. Otherwise, partial transfer will happen and the outcome is evident.

4.3.2 Substrate Treatment: 0.25% wt. KOH solution

Considering the previously demonstrated advantages of this treatment, implementation of the KOH solution step in the process was done. As shown in section ”Substrate Treatment: KOH solution”, glass substrates’ immersion was done for 20 seconds in a 0.25% wt. KOH solution aiming to promote a better adhesion of the NWs and subsequently obtain a better transfer yield.

Four transfers were done using flat squared PDMS with Ni NWs and flat glass substrates to verify the treatment’s influence on the transfer. Two of the transfers had a treated glass surface and the other two did not. Figure 4.18 shows the results of this exercise.

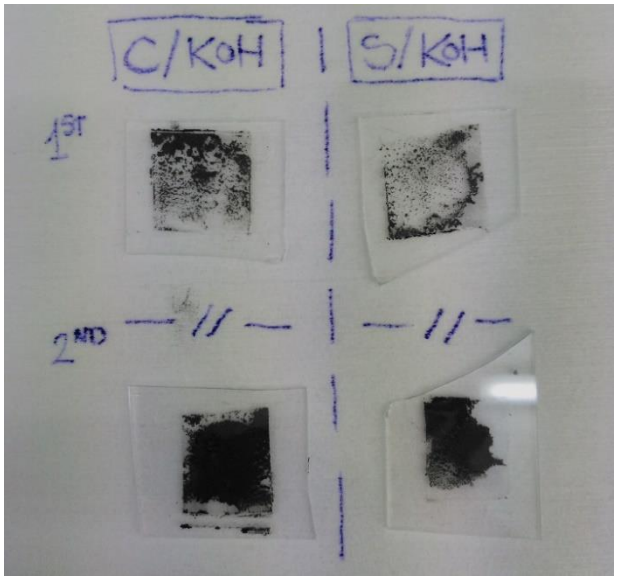

Figure 4.18 - Transfer trials to test KOH treatment influence. The left column is related to transfers on KOH-treated glass and the right column with no treatment.

There is a noticeable difference between using the treatment or not, especially in the second row, since a larger number of NWs was transferred. These samples were further analyzed through the Tabletop SEM, as shown in Figure 4.19.

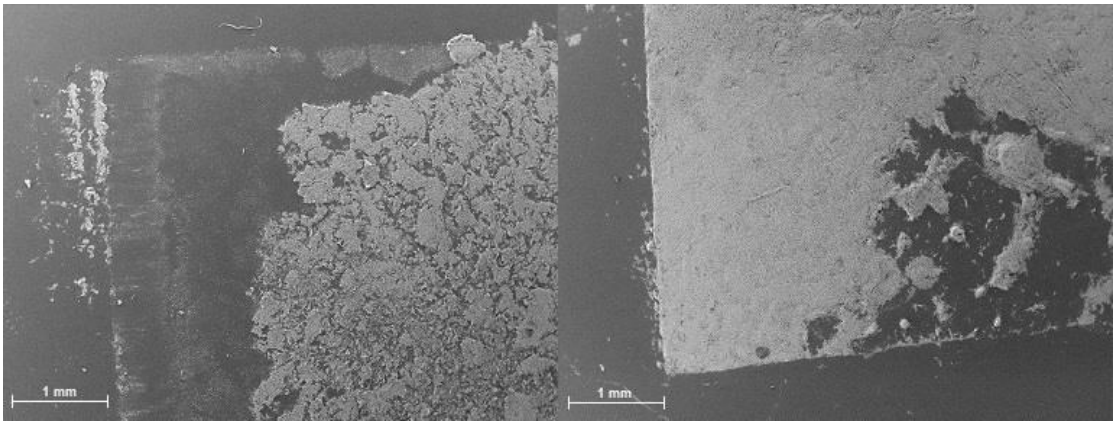

Figure 4.19 – SEM imaging and comparison between the second-row transfers in which a clear difference can be seen between the non-treated (left) and KOH-treated (right) samples.

Major improvements in terms of aspect-ratio were observed when the KOH solution was used. Pictures were taken from a corner of the transferred NWs and when the glass substrate is treated with KOH, an unquestionable higher aspect-ratio is attained. Likewise, in the case of non-treated

glass, NWs are more likely to aggregate during the transfer making the transferred layer is much less uniform, critical to the best success of the rubbing method.

4.3.3 Transfer Setup: Flat PDMS with Patterned Glass

New trials were done using previously patterned PR-coated glass substrates as transfer substrates and Ni NW-coated PDMS. The NW coating was done in two ways to study a possible NW alignment derived from mechanically-induced friction, so random rubbing and single-direction rubbing on the Ni NWs with the PDMS were executed, as shown in Annex P. Both transfer substrates were not submitted to HB. Additionally, NW excess was removed upon contact with another clean PDMS square, moving it in a single direction. Figure 4.20 depicts the transferred results.

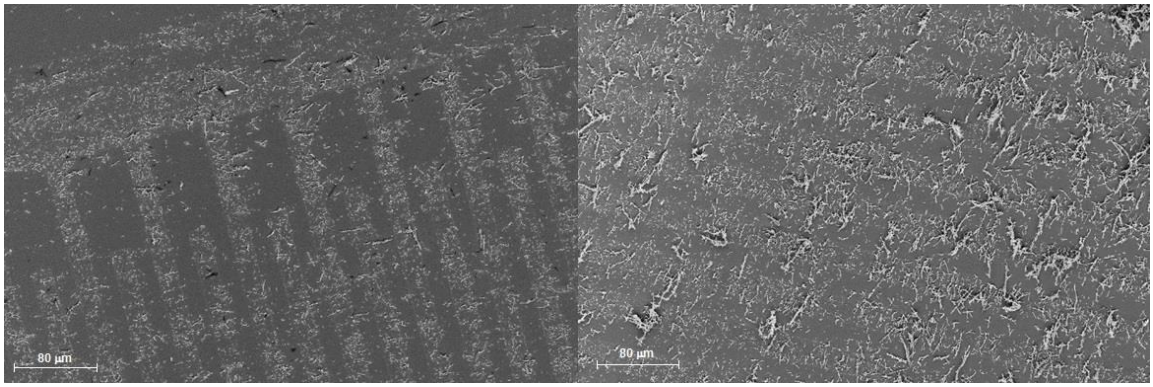

Figure 4.20 – SEM imaging of a Ni NW Transfer. Comparison is done between PDMS random rubbing (Left) and single direction rubbing (Right). PR tracks present a lighter color than the glass substrate.

From the observed results, NWs were not randomly oriented but were roughly aligned in a single direction. However, this alignment may not come from the rubbing but instead from the cleaning step. Since the removal of NW excess was done in one direction, it is most likely that this movement aligned the wires towards that same direction, making the rubbing motion irrelevant to the process. Likewise, most of the deposited NWs settled on top of the PR layer, proving an unsuccessful contact with the KOH-treated layer.

The same procedure was followed but this time samples differed in the PR-coating, which was either submitted to a HB step or not. This step was done at 115ºC for 60 seconds to check if the Reflow effect affected this transfer, since NWs could have a bigger probability of touching the glass substrate. Figure 4.21 establishes the comparison between both transfers.

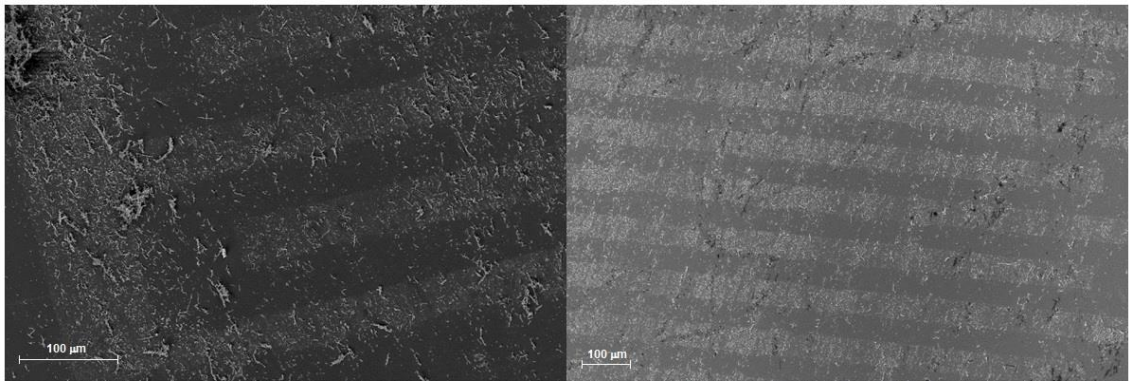

Figure 4.21 – SEM imaging of Ni NW transfer on top of patterned PR-coated glass, with a HB step (Left) and no HB whatsoever (Right). PR tracks present a lighter color than the glass substrate.

Reflow did not show any significant difference between both samples as there is no meaningful difference of NWD in the glass surface. Nevertheless, it is noticeable that the cleaning stage of

the process induces NW alignment, as mentioned before. Both PDMS squares used for the transfer rubbed the NWs in a single direction before the transfer stage.

Despite not making a good contact of the transferred wires with the glass substrate, PDMS transfer was successful and did not harm the PR tracks. NWs were spread mostly on top of the tracks and, when the excess was removed during the cleaning step, they embraced the same direction of the cleaning, probably due to mechanically-induced friction. However, the transferred NWs presented a wide range of lengths probably derived from the cleaning step done by hand, which could break the wires.

4.3.4 Transfer Setup: Patterned PDMS and Flat Glass

On the other way around, transfer with Patterned PDMS and flat glass substrates was tested. This aims to create conductive NW tracks using the same PDMS rubbing-and-transfer methodology. Designed patterns were done in Adobe™ Illustrator and are shown in Annex Q, where the black areas were engraved in the acrylic surface. Replicas of these where made with PDMS and used to perform transfer with Ni NWs.

Initially, these replicas were done by spin-coating PDMS on top of the patterned acrylic masters. Spin-coating replicas were done using the patterns found on Annex Q, on the left. Resulting PDMS came out as highly malleable thin layers of PDMS. The transferring process was identical to the one stated above, in which the PDMS replica is pressed against the NWs and put into contact with the flat glass substrate, having a layer of DI Water sandwiched between them, followed by freezing and subsequent PDMS peel-off and water evaporation. Results are shown in Figure 4.22 when the top-left pattern on Annex Q was used. It features 20x1 mm^2 tracks with a 1 mm spacing between each other.

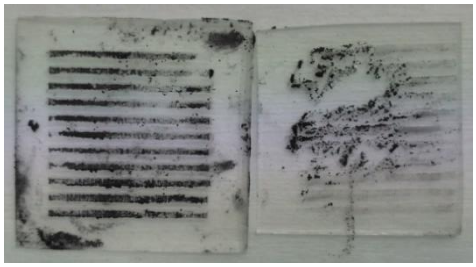

Figure 4.22 – Ni NW Transfer using a spin-coated PDMS replica (Left) and a flat glass (Right) as a transfer substrate.

The outcome of this transfer was disastrous and many factors can be pointed as main issues. First of all, the PDMS contact pressure was done bare-handed so the applied pressure is not uniform in the entire transfer area. Secondly, the replica is so soft that the water layer could deform it, creating water pockets inside, distorting the patterns and decreasing the freezing effectiveness. A clear demonstration of this effect is seen in Figure 4.22, on the right. Additionally, due to the replica's soft nature, PDMS successful detaching was hard since NW tracks were not successfully stuck to the glass surface.

Intending to improve this transfer, PDMS replicas were now done by pouring pre-cured PDMS on top of the acrylic masters in a plastic petri box, as pictured in Figure 4.23.

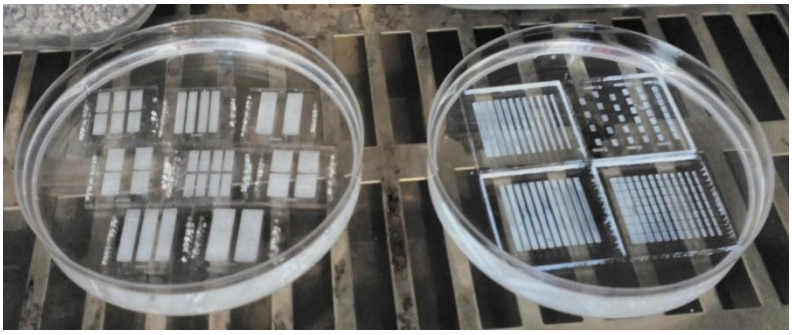

Figure 4.23 - PDMS replica production by pouring it on top of acrylic masters inside a plastic petri box.

These were then cut and demolded from the masters, generating thicker master's reproductions. Transfer was done using the same pattern as shown before in Figure 4.22 and some from the left petri box, on Figure 4.23. These tracks are 12 mm-long and 5 to 2 mm-wide with a 1 mm step. The outcome is pictured in Figure 4.24.

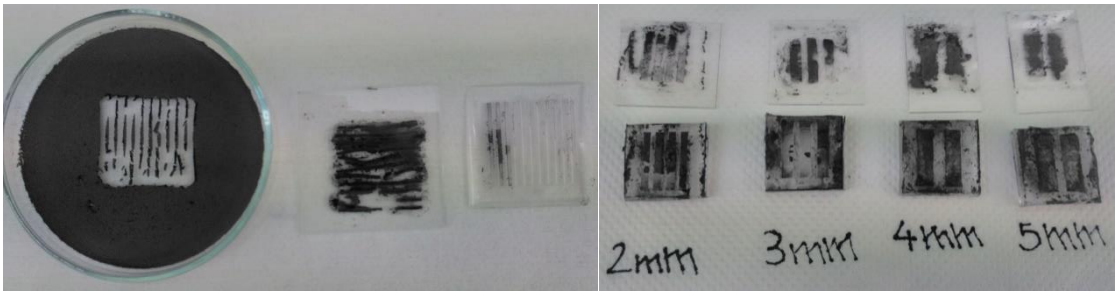

Figure 4.24 – Ni NW transfer using thicker PDMS replicas. Annex Q illustrates the used patterns.

NW tracks transfer was better using these thicker replicas. However, there was still a clear problem with PDMS pressure on top of the glass substrates and the used water volume. This way, the implementation of a hard element on the patterned PDMS's back was done with a 3D Printed Stamp. The patterned replica was fixed to the stamp's surface using a double-sided adhesive tape. This system was then used to press the settled NWs and subsequently press the glass surface. Likewise, the added stamp will improve the freezing step since its weight will contribute to a firmer contact. The transfers were now repeated as shown in Figure 4.25:

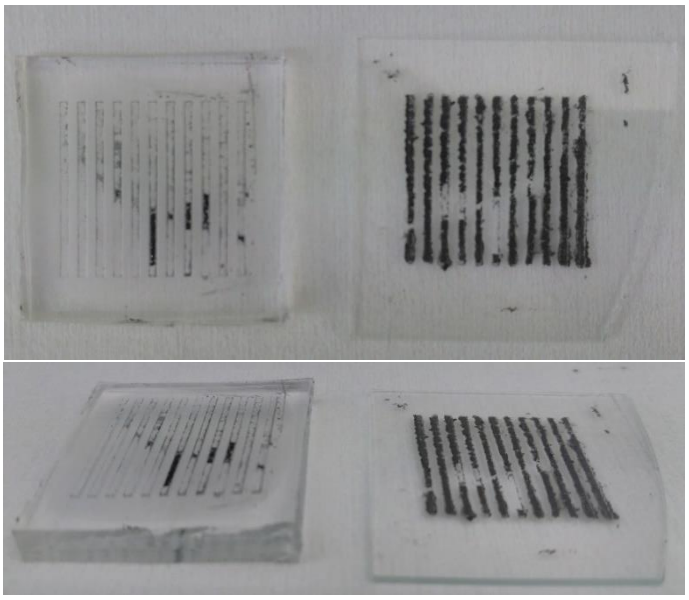

Figure 4.25 - Transfer repetition using a thicker PDMS, with the same pattern as in Figure 4.24, and a 3D-printed stamp.

Significant improvements were seen. Besides having most of the tracks transferred, the freezing-and-evaporation water step was more effective, probably due to a more effective pressure when freezing. The tracks are clearly separated from each other and most of them are almost complete.

However, when testing the track's electrical conductance, no good results were attained. Despite being apparently well adhered to the glass's surface, the NWs would come off if a probe was put into contact with them, aiming to perform an I-V measurement, for instance. Likewise, the patterned acrylic master's production also influenced the track's electrical measurements. The laser cutting machine engraves the acrylic board by vertical scanning, like shown in Annex R. This induced a lot of gaps in the transferred tracks, thus making it impossible to do an I-V sweep measurement. Figure 4.26 shows Optical Microscope analysis of an acrylic master and a PDMS replica of the initially designed patterns.

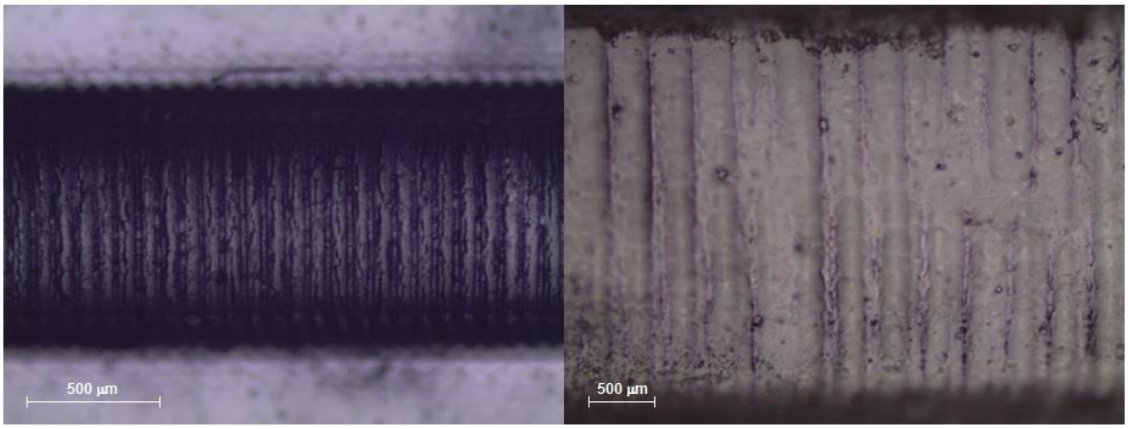

Figure 4.26 – Optical Microscope imaging of a laser engraved 1 mm-wide track on acrylic (Left), replicated with PDMS (Right). Horizontal engraving is illustrated, like shown in Annex R.

The designed patterns mixed with the scanning engraving motion from the laser cutting machine jeopardized the transferred tracks, that were divided into several parts. Consequently, only a few parts of the NWs are delivered when performing the transfer. Designs were redone (Annex S) so that the laser's engraving direction was collinear to the track's direction instead of being perpendicular to it, as seen in Figure 4.26. Figure 4.27 shows a transfer with the newly designed patterns only.

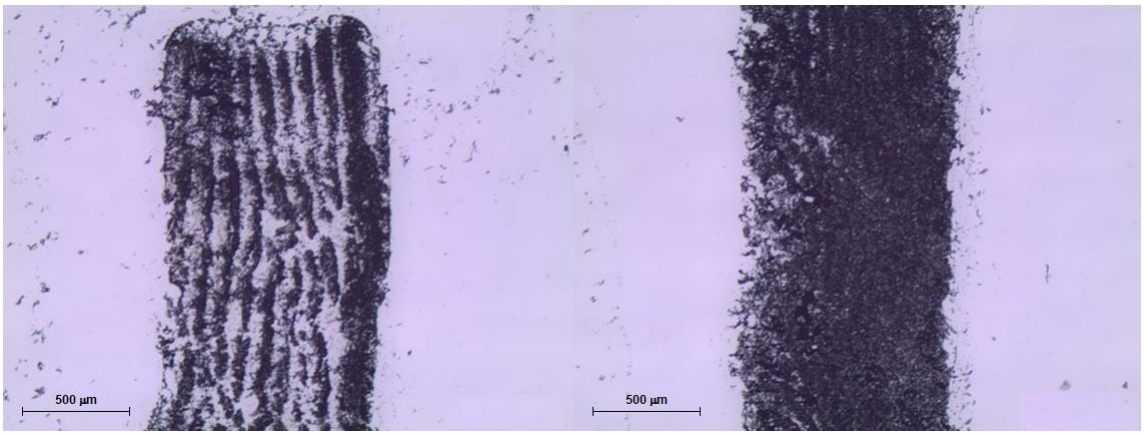

Figure 4.27 - Optical Microscope imaging of a NW transfer using the newly designed patterns. The left picture represents one edge of e transferred track and the right picture illustrates a part of a successfully transferred track.

Although it showed some better results, as it can be seen in Figure 4.27 (Right), transferred tracks were still strongly dependent of the laser's engraving and no major improvement was seen in terms of NW adhesion.

4.3.5 Transfer Setup Optimization: NW & Water Layer and Pattern Design

NW layer optimization was done to transfer uniform tracks to the transfer substrates. Tested NW weights were of: 5, 10, 15 and 20 mg dispersed in 5 mL of IPA. Figure 4.28 shows the difference between these 4 tests.

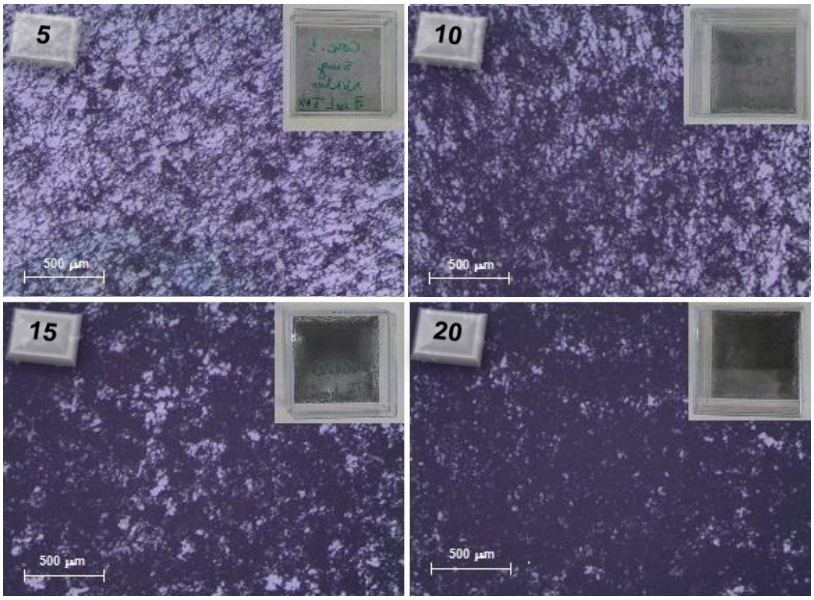

Figure 4.28 - Optical Microscope imaging of the NW layers with different NW masses: 5 mg on TLC, 10 mg on TRC, 15 mg on BLC and 20 mg on BRC.

Considering the apparently sufficient NWD to promote electron flow throughout the NW layer and also allied to a good transparency, masses of 5 mg and 10 mg of NWs were used from here on.

To perform more transfers using these weighted wires, the water layer also needed to be optimized. As mentioned in Chapter Methods, water spin-coating was considered to deposit a uniform water layer on the transfer substrate. However, substrate's high hydrophilicity was needed to maintain a stable water layer for enough time to put the NWs into contact with it and take it to the freezer. Since this water layer would evaporate rapidly, an also uniform glass treatment was done to increase its hydrophilicity, which was an UV Ozone Treatment. 15-minute and 30-minute treatment times were tested on glass and results were analyzed with CA measurements, as seen in Table 4.7.

Table 4.7 - CA measurements of 15-minute and 30-minute UV Ozone glass surface treatment.

	15 min. UV O_3 on Glass CA		**30 min. UV O_3 on Glass CA**	
Drop#	Left (˚)	Right (˚)	Left (˚)	Right (˚)
1	23.7	23.0	-	-
2	25.0	23.8	-	-
3	23.2	23.3	-	-
4	23.6	24.4	-	-
Mean (˚)	23.8		-	
Std Dev (˚)	0.7		-	

30-minute UV Ozone treatment Cas are not displayed since the software was unable to read them due to the high hydrophilicity shown, thus making this treatment the chosen one.

New transfer trials were done to test these new process features using the previously upgraded patterned PDMS as seen in Figure 4.27. 5 mg of Ni NWs were used in the transfer. Figure 4.29 shows the outcome.

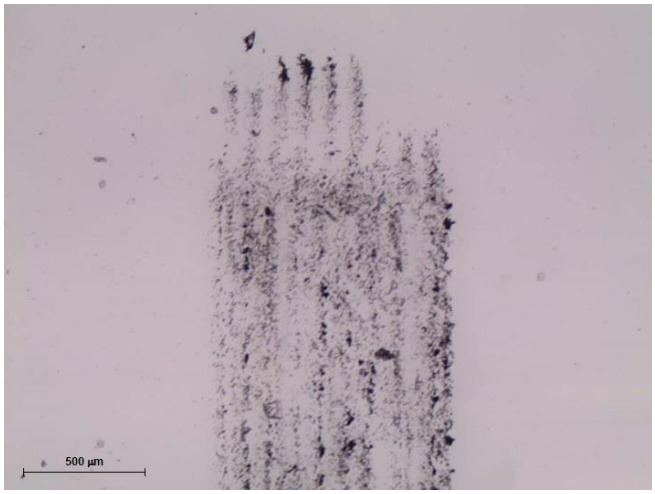

Figure 4.29 - Optical Microscope imaging of a 5 mg NiNW transfer using Patterned PDMS and spin-coating water on top of a glass substrate, previously submitted to a 30-minute UV Ozone surface treatment.

The NW mass revealed to be extremely low for this transfer process since faulty tracks were transferred. Additionally, laser engraving becomes more prominent with these low masses of NWs, compared to Figure 4.27 where transferred NWs' mass was not weighted.

In order to further optimize the PDMS replica, and acrylic patterned master was done but with a tweak: instead of engraving the pattern, it was cut from one side to another of the acrylic. Figure 4.30 establishes the difference.

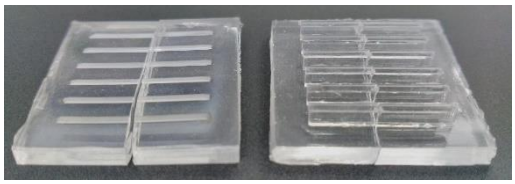

Figure 4.30 - PDMS molds of the same pattern, in which one was replicated from a engraved acrylic master (Left) and the other from a cut acrylic master (Right).

These replicas analyzed through the Tabletop SEM to inspect the surface roughness on their tracks. Figure 4.31 pictures the comparison.

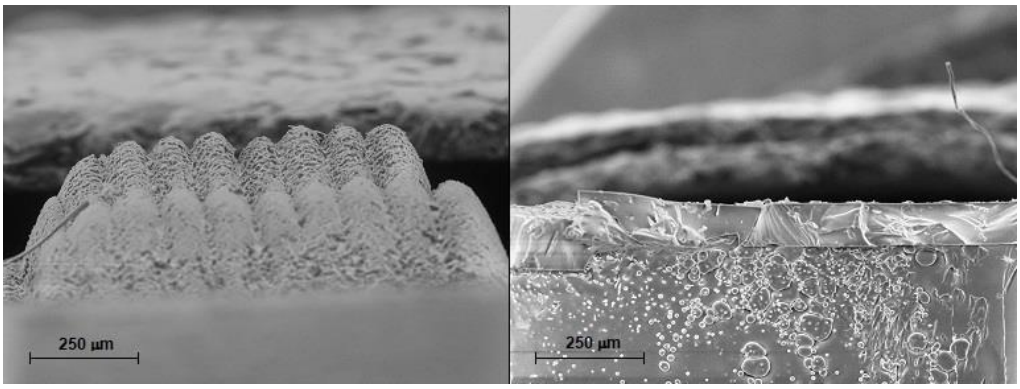

Figure 4.31 - SEM analysis of PDMS replica's surface roughness , in which one was replicated from an engraved acrylic master (Left) and the other from a cut acrylic master (Right).

As it shows, the laser engraving mode is very prejudicial to the transfer's yield since only a few parts of the whole track will contact the glass's surface firmly. On the other hand, the replica of the cut acrylic master presented a smooth track surface, much better than the engraved.

Therefore, new acrylic masters were done. The PDMS replica on Figure 4.30 (Right) was not used since the tracks were too high. So, in order to obtain smooth PDMS tracks for the transfer, acrylic masters were done in the laser cutting machine, as presented in Figure 4.32.

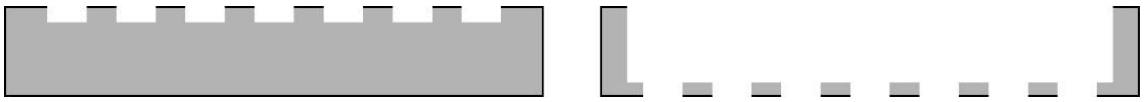

Figure 4.32 - Comparison between the inicial acrylic master (Left) and the optimized acrylic master (Right).

The PDMS replicas were done the same way, i.e. by putting the master inside a petri box and pouring pre-cured PDMS on top of it, and demolding was a bit trickier than the initial acrylic masters but still moderately easy. Figure 4.33 shows a transfer using these new molds. This time, 10 mg of Ni NWs were transferred and water spin-coating was also done.

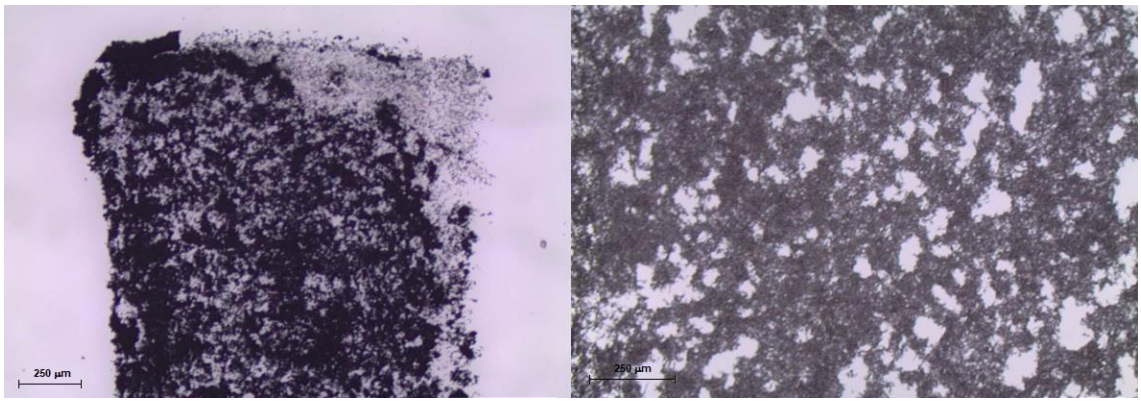

Figure 4.33 - Optical Microscope imaging of a Ni NW transfer on glass using PDMS replica of the newly optimized acrylic master.

These tests showed promising results. Despite having a lot of gaps in the transferred tracks, its form was very similar to the acrylic master's. 10 mg of wires also seemed more adequate to the process compared to 5 mg, which presented more gaps and most of the times wider. Conductive Ni NWs tracks were created but the issue regarding their adhesion to the surface is still problematic, preventing an electrical characterization of the tracks.

ZTO NW transfer was also done using the same procedure and NW mass. Figure 4.34 depicts the outcome.

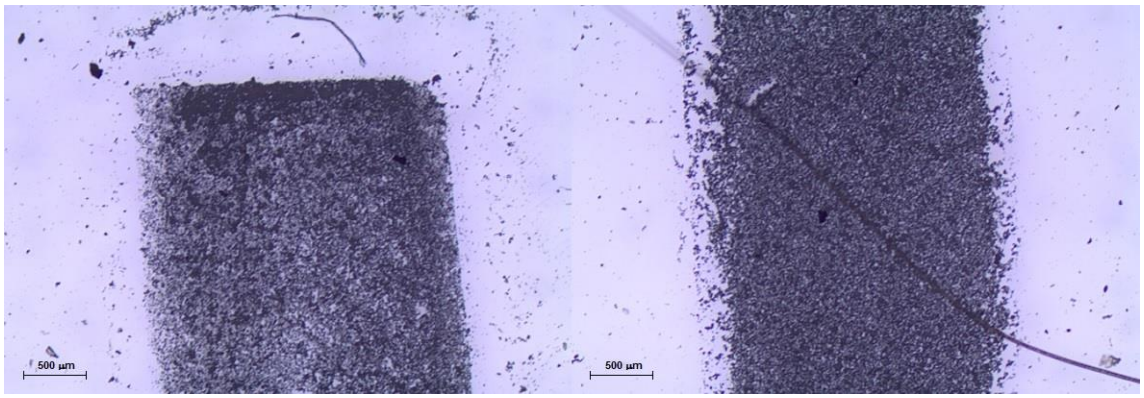

Figure 4.34 - Optical Microscope imaging of a ZTO NW transfer on glass using the same PDMS replica.

The semiconductor wires were also transferred to the glass surface but with inferior yield. When transferring the Ni NWs, most of the tracks were successfully delivered but it was not the case with ZTO. One of the reasons behind this lower yield could be the lack of pressure during the freezing step.

4.3.6 Flexible Substrate: PEN

Transfers were mostly done on glass, which is a rigid substrate. However, it is of utmost importance to test this method in a flexible substrate, like PEN (Polyethylene Naphthalate), to inspect this method's substrate compatibility. Using the same elements as the previous experiment, a NW transfer was done. However, the PEN substrate must be prepared properly so that it is compatible with the methodologies used. For instance, its surface must be highly hydrophilic. Different UV Ozone surface treatment times were tested and analyzed with CA measurements, just like the glass substrate. A 60-minute treatment was adequate to the PEN surface, manifesting a highly hydrophilic character, as is noticed in Figure 4.35.

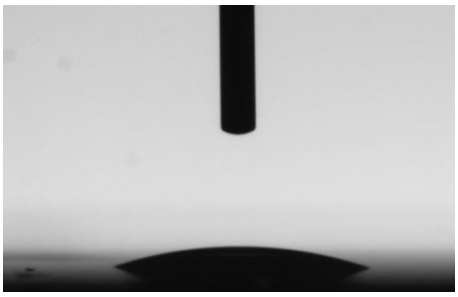

Figure 4.35 - CA measure of the 60-minute UV Ozone treated PEN surface.

Additionally, due to PEN's flexibility, a glass backing was attached to it by using a double-sided adhesive tape to grip each corner of the flexible substrate to the glass. This feature was added due to the water spin-coating step, in which the substrate must be as flat as possible.

Transfer trial is pictured in Figure 4.36 and compared with the glass surface.

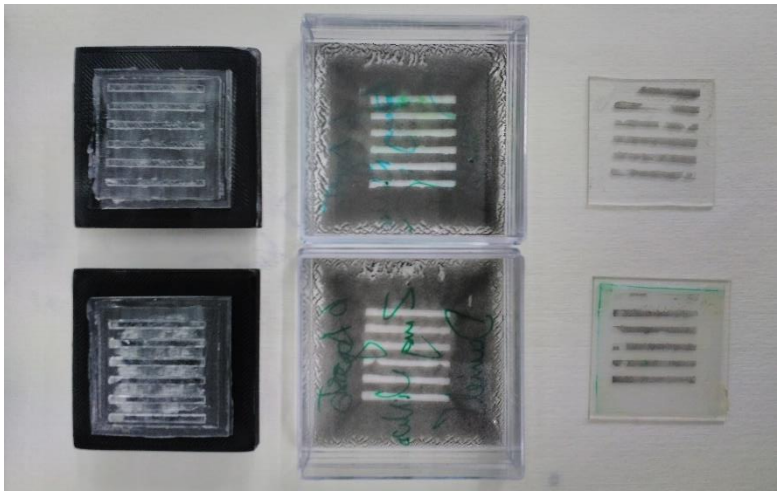

Figure 4.36 - Ni NW transfer with optimized features on a glass surface (Top) and a PEN substrate (Bottom).

This trial proved to be successful when transferring to a flexible substrate like PEN. An identical NW track uniformity was attained and its morphological inspection was done using the Optical Microscope, as pictured in Figure 4.37.

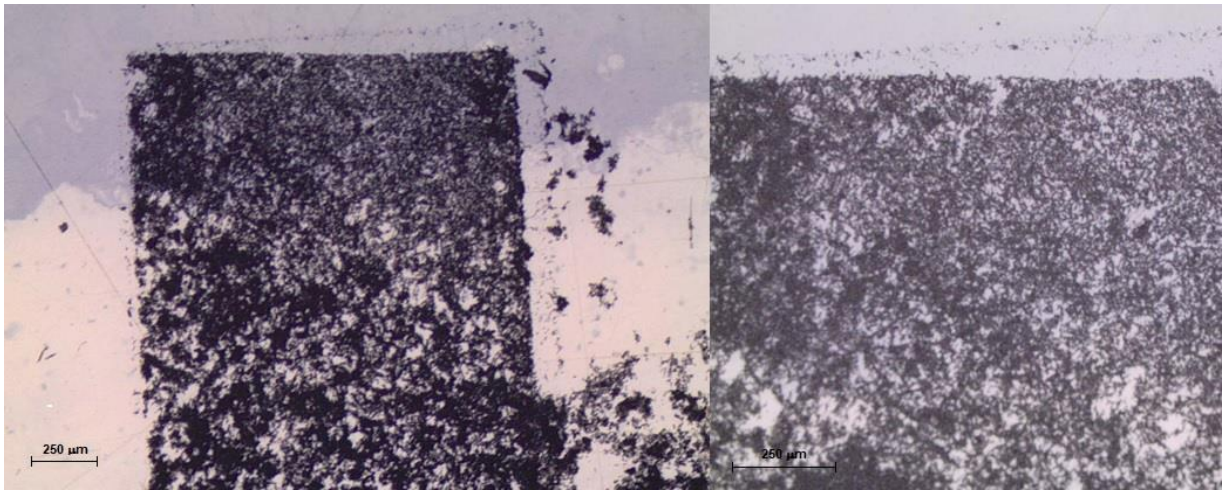

Figure 4.37 - Optical Microscope imaging of a Ni NW transfer trial done on top of a PEN substrate.

Figure 4.37 showed that transferring to the PEN substrate was a confirmed success since it presented identical consistency and the transfer to the glass substrate, pictured in Figure 4.33.

Accordingly, ZTO NW transfer was also attained on top of a PEN substrate using the same methodology. Figure 4.38 pictures the results.

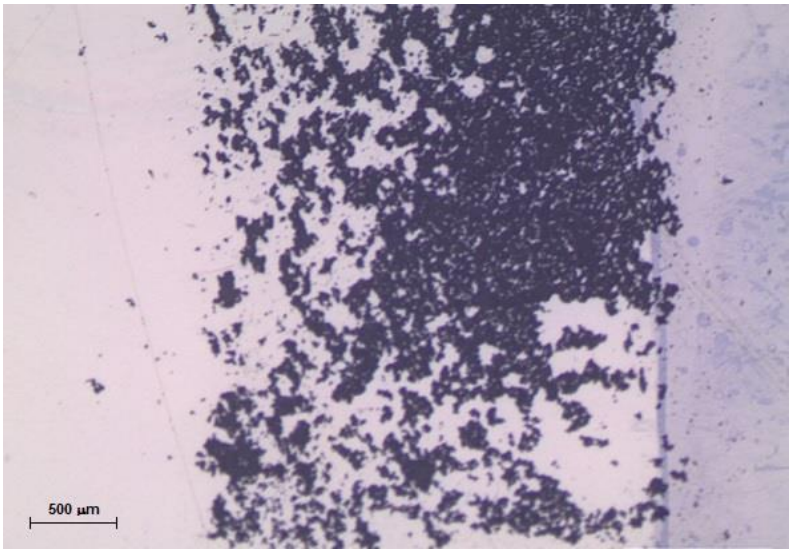

Figure 4.38 - Optical Microscope imaging of a ZTO NW transfer trial done on top of a PEN substrate.

Despite occurring NW transfer, the outcome was not nearly as good as the Ni NW transfer. Pressure when freezing could also be the main cause of the unsuccessful test.

However, this methodology was considered compatible with this flexible substrate and probably compatible with a lot of other substrates since it does not rely on their composition but rather on their surface hydrophilicity. Study of the transfer pressure is critical to establish comparison with the obtained results in Figures 4.37 and 4.38.

5. CONCLUSION AND FUTURE PERSPECTIVES

5.1 Conclusion

NCA's reported results showed an outstanding potential as far as transferring aligned NW arrays was concerned. Despite obtaining adequate PR thickness and substrate functionalization, transfer trials turned out unsuccessful. This can be explained through the fact that crucial elements of the process could not be mimicked like the transfer speed and patterns' dimensions, as explained in the Chapter Results. Also, average ZnO NWs length was very different from the reported Si NWs length, which could also be one of the main problems. Considering all the referred drawbacks, the reproduction of NCA was consequently unreliable.

On the other hand, Rubbing showed great promise when transferring random NW arrays. Besides being a low cost and simple method, it also provided the opportunity to deposit NW meshes at room temperature on rigid and flexible substrates, glass and PEN respectively. Although substrate's surface treatment, PDMS production and NW layer settling are lengthy stages of this process, the transfer methodology itself is very fast, taking up to roughly 10 minutes, in which the freezing step takes approximately 5 minutes. Furthermore, this method does not depend on the nanostructure compounds nor the substrate's composition, which is a very important asset. Additionally, the ability to be integrated in large-area production of rigid and flexible devices seems attainable since it does not depend on the pattern dimensions and feature sizes but rather on the adequate and accurate PDMS contact pressure with the substrate's surface throughout the process and the water freezing time.

5.2 Future Perspectives

In order to successfully reproduce NCA, one must assemble a system in which is possible to do NW transfers at reported speeds, 2-20 mm/minute, and pressure, 2-6 N/cm^2. Furthermore, the PR layer needs to be optimized aiming to increase its CA and to diminish any sort of interactions between its surface and the combed NWs, or another type of PR is to be considered. If the reproduction of this process is accomplished accordingly to the reported results, the transferred NWD should be ≈2 NW/μm and it is of utmost importance to improve its yield so that more devices can be assembled per transfer.

If a shape-memory polymer such as Polystyrene (PS), is used as a transfer substrate, NWD can be raised by ≈300% maximum. Using 2 clamps on 2 opposite sides of the substrate to apply heat above PS's glass transition temperature, uniaxial shrinkage of the polymer will occur thus bringing the aligned NW closer to each other without jeopardizing their alignment. PS can then be removed with a toluene solution, leaving the NWs behind.[60] Figure 5.1 depicts the described process.

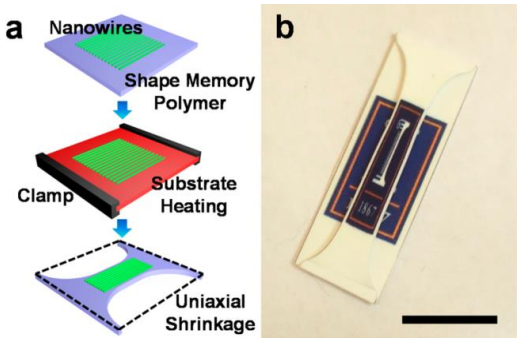

Figure 5.1 - PS shrinking to increase NWD using two heated clamps in which (a) shows the important stages of the process and (b) establishes a comparison between uniaxially deformed PS substrate on top of a non-heated PS substrate. Scale bar is of 2 cm.[60]

As far as Rubbing is concerned, improvements on contact pressure between the PDMS and substrate will most likely improve the method's yield. More importantly, nanostructure/substrate interface optimization needs to be attained in order to study the transferred patterns properties and eventually, assemble devices with them.

A decrease on patterned PDMS feature sizes would be reasonable to check the method's ability to transfer nanopatterns. Through the use of sophisticated lithography techniques like DUV OL or EBL, a master mold with nanoscale features can be produced and PDMS replicas can be made out of it.[16] Following the same procedure as Rubbing, nanoscale patterns could be easily transferred to a wide variety of substrates, , mimicking an ultra-low cost micro-contact printing tool. However, an automated system needs to be assembled so that nanopatterns are properly transferred. Figure 5.2 shows the replication of a produced master through OL.

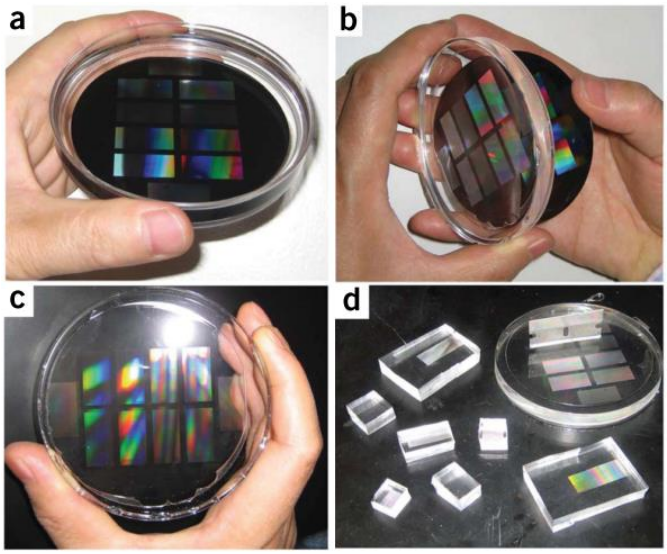

Figure 5.2 - PDMS replication of a OL-produced master. The stages of this process are identical to Rubbing. From (a) to (c), PDMS demolding stages are shown after the curing step, where the polymer is patternized by a master mold. This process is identical to the explained on as described[16]

7. BIBLIOGRAPHY

1. Moore, G. E. Cramming more components onto integrated circuits (Reprinted from Electronics, pg 114-117, April 19, 1965). *Proc. Ieee* **86,** 82–85 (1965).
2. Biswas, A. *et al.* Advances in top-down and bottom-up surface nanofabrication: Techniques, applications & future prospects. *Adv. Colloid Interface Sci.* **170,** 2–27 (2012).
3. Fan, P., Zhong, M., Bai, B., Jin, G. & Zhang, H. Large scale and cost effective generation of 3D self-supporting oxide nanowire architectures by a top-down and bottom-up combined approach. *RSC Adv.* **6,** 45923–45930 (2016).
4. Papadopoulos, C. *Nanofabrication: Principles and Applications*. (Springer International Publishing, 2016). doi:10.1007/978-3-319-31742-7
5. Feldman, M. *Nanolithography: The Art of Fabricating Nanoelectronic and Nanophotonic Devices and Systems*. (Woodhead Publishing Limited, 2014). doi:10.1533/9780857098757
6. Xia, Y., Rogers, J. A., Paul, K. E. & Whitesides, G. M. Unconventional Methods for Fabricating and Patterning Nanostructures. *Chem. Rev.* **99,** 1823–1848 (1999).
7. Rogers, J. A. & Nuzzo, R. G. Recent progress in soft lithography. in *Materials Today* **8,** 50–56 (2005).
8. Badaroglu, M. More Moore Scaling: opportunities and inflection points. in *Bridging the Research Gap between Emerging Architectures and Devices* (ITRS Emerging Research Device (ERD) Meeting, 2015).
9. Thompson, S. E. & Parthasarathy, S. Moore's law: the future of Si microelectronics. *Mater. Today* **9,** 20–25 (2006).
10. Cui, Z. *Nanofabrication*. (Springer US, 2008). doi:10.1007/978-0-387-75577-9
11. Walia, S. *et al.* Flexible metasurfaces and metamaterials: A review of materials and fabrication processes at micro- and nano-scales. *Appl. Phys. Rev.* **2,** (2015).
12. Huang, W., Yu, X., Liu, Y., Qiao, W. & Chen, L. A review of the scalable nano-manufacturing technology for flexible devices. *Front. Mech. Eng.* **12,** 99–109 (2017).
13. Khan, S., Lorenzelli, L. & Dahiya, R. S. Technologies for printing sensors and electronics over large flexible substrates: A review. *IEEE Sens. J.* **15,** 3164–3185 (2015).
14. Kish, L. B. End of Moore's law: Thermal (noise) death of integration in micro and nano electronics. *Phys. Lett. Sect. A Gen. At. Solid State Phys.* **305,** 144–149 (2002).
15. Wang, K. L. Issues of Nanoelectronics: A Possible Roadmap. *J. Nanosci. Nanotechnol.* **2,** 235–266 (2002).
16. Qin, D., Xia, Y. & Whitesides, G. M. Soft lithography for micro- and nanoscale patterning. *Nat. Protoc.* **5,** 491–502 (2010).
17. Loo, Y. L., Willett, R. L., Baldwin, K. W. & Rogers, J. A. Additive, nanoscale patterning of metal films with a stamp and a surface chemistry mediated transfer process: Applications in plastic electronics. *Appl. Phys. Lett.* **81,** 562–564 (2002).
18. Menard, E., Bilhaut, L., Zaumseil, J. & Rogers, J. A. Improved surface chemistries, thin film deposition techniques, and stamp designs for nanotransfer printing. *Langmuir* **20,** 6871–6878 (2004).
19. Wang, Z. L. *Nanowires and Nanobelts: Materials, Properties and Devices. Volume 1: Metal and Semiconductor Nanowires, Volume 1*. **1,** (2013).
20. Fan, H. J., Werner, P. & Zacharias, M. Semiconductor nanowires: From self-organization to patterned growth. *Small* **2,** 700–717 (2006).

21. Chang, P.-C. *et al.* Characterization ZnO Nanowires Synthesized by Vapor Trapping CVD Method . *Microsc. Microanal.* **10,** 5133–5137 (2004).

22. Zhang, A., Zheng, G. & M. Lieber, C. *Nanowires: Building Blocks for Nanoscience and Nanotechnology*. (Springer International Publishing, 2016). doi:10.1007/978-3-319-41981-7

23. Luo, L., Zhang, Y., Mao, S. S. & Lin, L. Fabrication and characterization of ZnO nanowires based UV photodiodes. *Sensors Actuators, A Phys.* **127,** 201–206 (2006).

24. Bulgarini, G. *et al.* Avalanche amplification of a single exciton in a semiconductor nanowire. *Nat. Photonics* **6,** 455–458 (2012).

25. Hannon, J. B., Kodambaka, S., Ross, F. M. & Tromp, R. M. The influence of the surface migration of gold on the growth of silicon nanowires. *Nature* **440,** 69–71 (2006).

26. Wu, Y. & Yang, P. Direct observation of vapor-liquid-solid nanowire growth. *J. Am. Chem. Soc.* **123,** 3165–3166 (2001).

27. Hochbaum, a I., Fan, R., He, R. R. & Yang, P. D. Controlled growth of Si nanowire arrays for device integration. *Nano Lett.* **5,** 457–460 (2005).

28. Wang, Y., Schmidt, V., Senz, S. & Gösele, U. Epitaxial growth of silicon nanowires using an aluminium catalyst. *Nat. Nanotechnol.* **1,** 186–189 (2006).

29. Kolasinski, K. W. Catalytic growth of nanowires: Vapor-liquid-solid, vapor-solid-solid, solution-liquid-solid and solid-liquid-solid growth. *Curr. Opin. Solid State Mater. Sci.* **10,** 182–191 (2006).

30. Vayssieres, L. Growth of arrayed nanorods and nanowires of ZnO from aqueous solutions. *Adv. Mater.* **15,** 464–466 (2003).

31. Yu, H. & Buhro, W. E. Solution-liquid-solid growth of soluble GaAs nanowires. *Adv. Mater.* **15,** 416–419 (2003).

32. Li, Q. C. *et al.* Fabrication of ZnO Nanorods and Nanotubes in Aqueous Solutions - Chemistry of Materials. *Chem. Mater.* 1001–1006 (2005). doi:10.1021/cm048144q

33. Greene, L., Yuhas, B. & Law, M. Solution-grown zinc oxide nanowires. *Inorg. Chem.* **45,** 7535–43 (2006).

34. Han, Y. J., Kim, J. M. & Stucky, G. D. Preparation of noble metal nanowires using hexagonal mesoporous silica SBA-15. *Chem. Mater.* **12,** 2068–2069 (2000).

35. Yan, H. DNA-Templated Self-Assembly of Protein Arrays and Highly Conductive Nanowires. *Science (80-.).* **301,** 1882–1884 (2003).

36. Song, J., Lim, S., Lim, J. S. and S., Song, J. & Lim, S. Effect of Seed Layer on the Growth of ZnO Nanorods. *J. Phys. Chem. C* **111,** 596–600 (2007).

37. Guo, W., Zhang, M., Banerjee, A. & Bhattacharya, P. Catalyst-free InGaN/GaN nanowire light emitting diodes grown on (001) silicon by molecular beam epitaxy. *Nano Lett.* **10,** 3356–3359 (2010).

38. Park, W. I., Kim, D. H., Jung, S. W. & Yi, G. C. Metalorganic vapor-phase epitaxial growth of vertically well-aligned ZnO nanorods. *Appl. Phys. Lett.* **80,** 4232–4234 (2002).

39. Park, W. Il, Yi, G. C., Kim, M. & Pennycook, S. J. ZnO nanoneedles grown vertically on Si substrates by non-catalytic vapor-phase epitaxy. *Adv. Mater.* **14,** 1841–1843 (2002).

40. Yerushalmi, R., Jacobson, Z. A., Ho, J. C., Fan, Z. & Javey, A. Large scale, highly ordered assembly of nanowire parallel arrays by differential roll printing. *Appl. Phys. Lett.* **91,** 114–117 (2007).

41. Zhu, G., Yang, R., Wang, S. & Wang, Z. L. Flexible high-output nanogenerator based on lateral ZnO nanowire array. *Nano Lett.* **10,** 3151–3155 (2010).

42. Yu, G., Cao, A. & Lieber, C. M. Large-area blown bubble films of aligned nanowires and carbon nanotubes. *Nat Nanotechnol* **2,** 372–377 (2007).

43. Schneider, G. F., Calado, V. E., Zandbergen, H., Vandersypen, L. M. K. & Dekker, C. Wedging transfer of nanostructures. *Nano Lett.* **10,** 1912–1916 (2010).

44. Yao, J., Yan, H. & Lieber, C. M. A nanoscale combing technique for the large-scale assembly of highly aligned nanowires. *Nat Nanotechnol* **8,** 329–335 (2013).

45. Biswas, P. *et al.* Low temperature solution process-based defect-induced orange-red light emitting diode. *Sci. Rep.* **5,** 17961 (2015).

46. Kumar, A. & Whitesides, G. M. Features of gold having micrometer to centimeter dimensions can be formed through a combination of stamping with an elastomeric stamp and an alkanethiol 'ink' followed by chemical etching. *Appl. Phys. Lett.* **63,** 2002–2004 (1993).

47. Zhang, Y., Ram, M. K., Stefanakos, E. K. & Goswami, D. Y. Synthesis, Characterization, and Applications of ZnO Nanowires. *J. Nanomater.* **22,** (2012).

48. Tereshchenko, A. *et al.* Optical biosensors based on ZnO nanostructures: Advantages and perspectives. A review. *Sensors Actuators, B Chem.* **229,** 664–677 (2016).

49. Gonzalez-Valls, I. & Lira-Cantu, M. Vertically-aligned nanostructures of ZnO for excitonic solar cells: a review. *Energy Environ. Sci.* **2,** 19–34 (2008).

50. Yoo, B., Rheem, Y., Beyermann, W. P. & Myung, N. V. Magnetically assembled 30 nm diameter nickel nanowire with ferromagnetic electrodes. *Nanotechnology* **17,** 2512–2517 (2006).

51. Samardak, A. S. *et al.* High-density nickel nanowire arrays for data storage applications. *J. Phys. Conf. Ser.* **345,** 12011 (2012).

52. Park, J. *et al.* High-Performance Zinc Tin Oxide Semiconductor Grown by Atmospheric-Pressure Mist-CVD and the Associated Thin-Film Transistor Properties. *ACS Appl. Mater. Interfaces* **9,** 20656–20663 (2017).

53. Wang, L., Zhang, X., Liao, X. & Yang, W. A simple method to synthesize single-crystalline Zn 2 SnO 4 (ZTO) nanowires and their photoluminescence properties. *Nanotechnology* **16,** 2928 (2005).

54. Maiti, U. N., Maiti, S., Thapa, R. & Chattopadhyay, K. K. Flexible cold cathode with ultralow threshold field designed through wet chemical route. *Nanotechnology* **21,** (2010).

55. Kong, Y. Y., Pang, S. C. & Chin, S. F. Facile synthesis of nickel nanowires with controllable morphology. *Mater. Lett.* **142,** 1–3 (2015).

56. Li, Z. *et al.* Vertically building Zn2SnO4 nanowire arrays on stainless steel mesh toward fabrication of large-area, flexible dye-sensitized solar cells. *Nanoscale* **4,** 3490 (2012).

57. Merck Perfomance Materials. Technical Data Sheet Technisches Datenblatt - AZ ECI 3000 Photoresist. **49,** (1990).

58. Domingos, I. D. Nickel nanowire synthesis for next-generation transparent conductors. (2016).

59. Mack, C. *Fundamental Principles of Optical Lithography*. *Fundamental Principles of Optical Lithography* (Wiley, 2007). doi:10.1002/9780470723876

60. Nam, S. Assembly and Densification of Nanowire Arrays via Shrinkage. *Nano Lett.* 3304–3308 (2014).

8. ANNEXES

Annex A – Lithography Resolution in the course of time.[9]

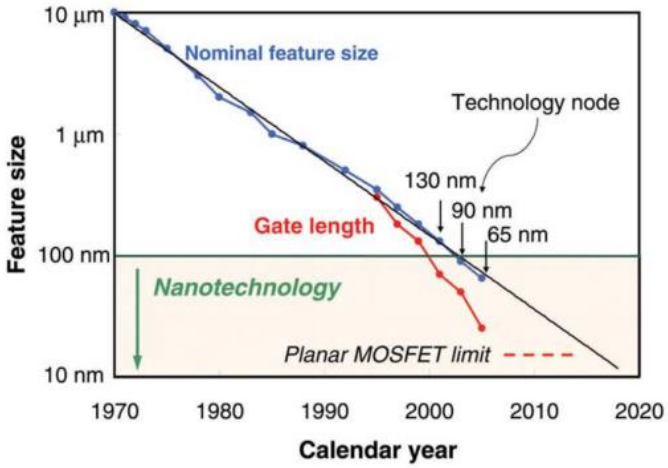

Annex B – VLS NW growth stages.[26]

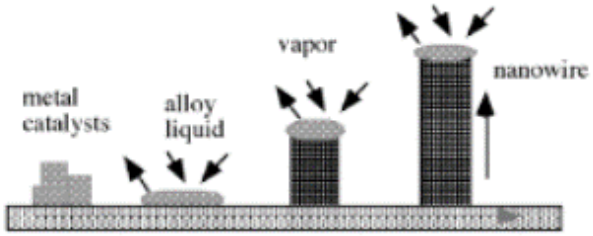

Annex C – Synthesized NW compounds by VLS mechanism.[20]

Table 1. Different semiconductor/metal combinations and growth methods for nanowires.

NW material	Source	Metal catalyst	Growth process[a]
Si	$SiCl_4$	Au	CVD
Si	$SiCl_4$	Au, Ag, Cu, Pt	CVD
Si, Ge	SiH_4, GeH_4	Au	CVD
Si	SiH_4	Au	CVD
Si, Ge		Fe, Si/Fe, Ge/Fe	PLD
Si	Si_2H_6	Au	CBE
GaAs	GaAs/Au	Au	PLD
InP	InP/Au	Au	PLD
CdSe	CdSe/Au	Au	PLD
Si	Si	Ga	microwave plasma
GaAs	Et_3Ga, Bu_3As	Au	CBE
ZnO	ZnO, C	Au	evaporation
Si	Si	Au	MBE
Si	SiO	Au	evaporation
Si	silyl radicals	Ga	microwave plasma etching
Si	SiH_4 or SiH_2Cl_2	Ti	CVD
GaAs/GaP	GaAs/GaP	Au	PLD
GaAs/InAs	Me_3Ga, Bu_3As, Me_3In	Au	CBE
Si/SiGe	$SiCl_4$	Au	Si: CVD; Ge: PLD

[a] PLD: pulsed laser deposition; CBE: chemical beam epitaxy.

Annex D – DRP setup (Left) and transfer outcomes in various substrates (Right).[40]

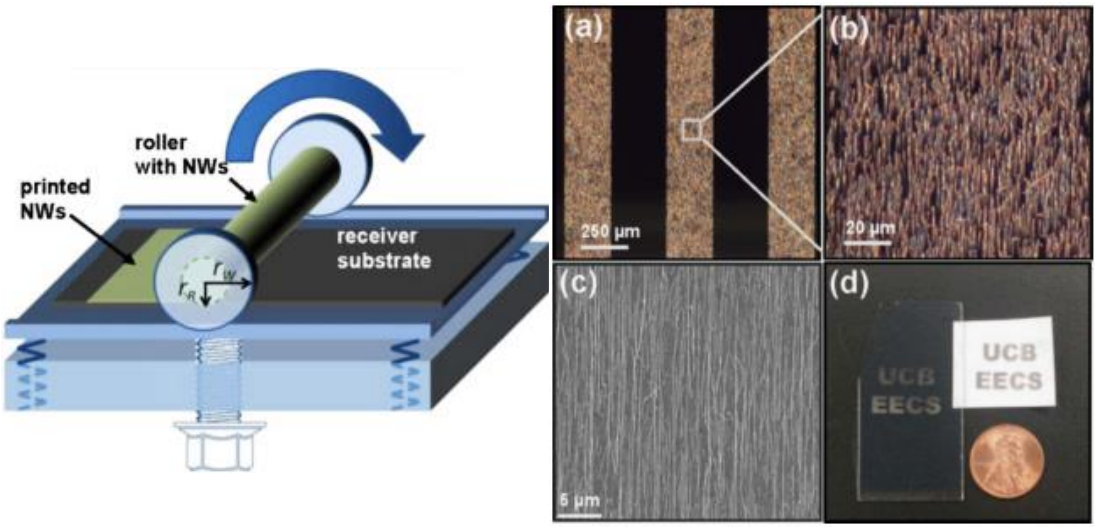

Annex E – SP setup (Left) where the movable stage's axis is represented. (a) shows a close-up of the method's elements, (b) the ZnO NWs growth substrate and (c) the outcome transfer from SP.[41]

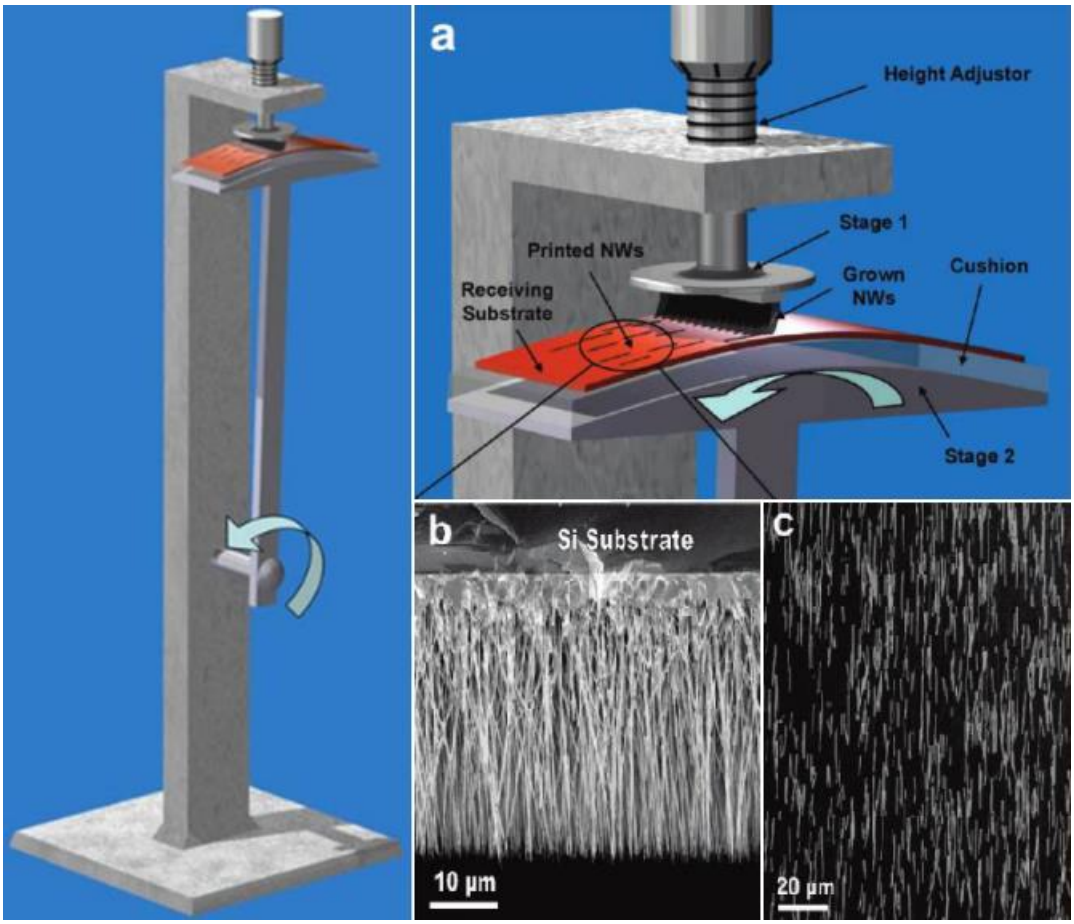

Annex F – BBF procedure. (a) represents de mixture of THF, Epoxy resin and the NWs/NTs, (b) the polymer bubble blowing step and (c) the outcome of the transfer in various kinds of substrates.[42]

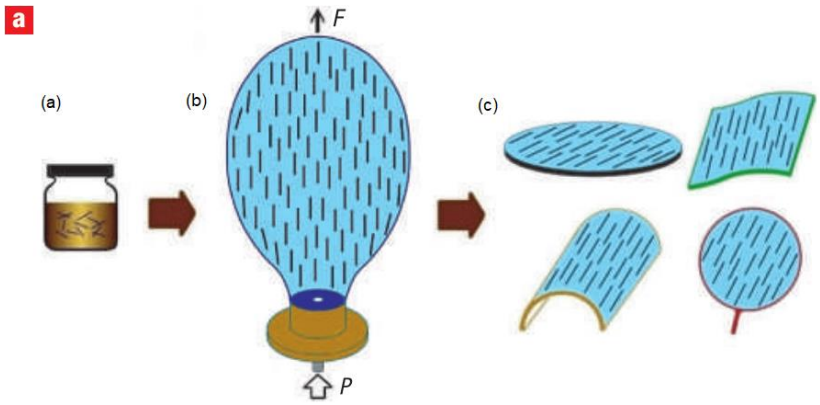

Annex G – Transferred SiNWs to a Si wafer (a), a curved surface (b) and a flexible plastic substrate (c). Note that the curved substrate is a 6 cm-long cylinder half with a diameter of 2.5 cm and the plastic substrate is 225x300 mm^2. Scale bar is set to (a) 2 μm and (b) 10 μm.[42]

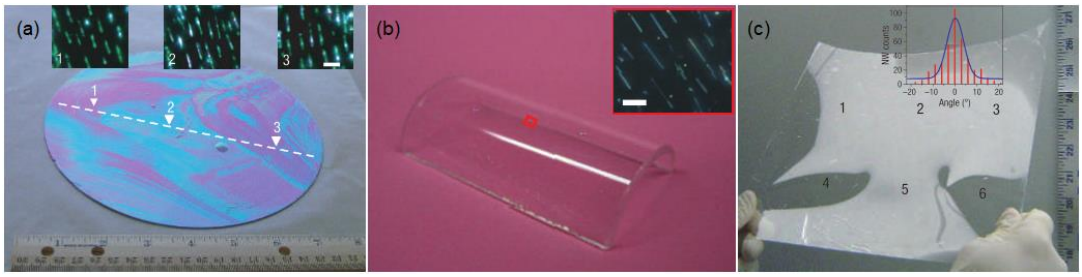

Annex H – WW transfer methodology from (i) to (v).[43]

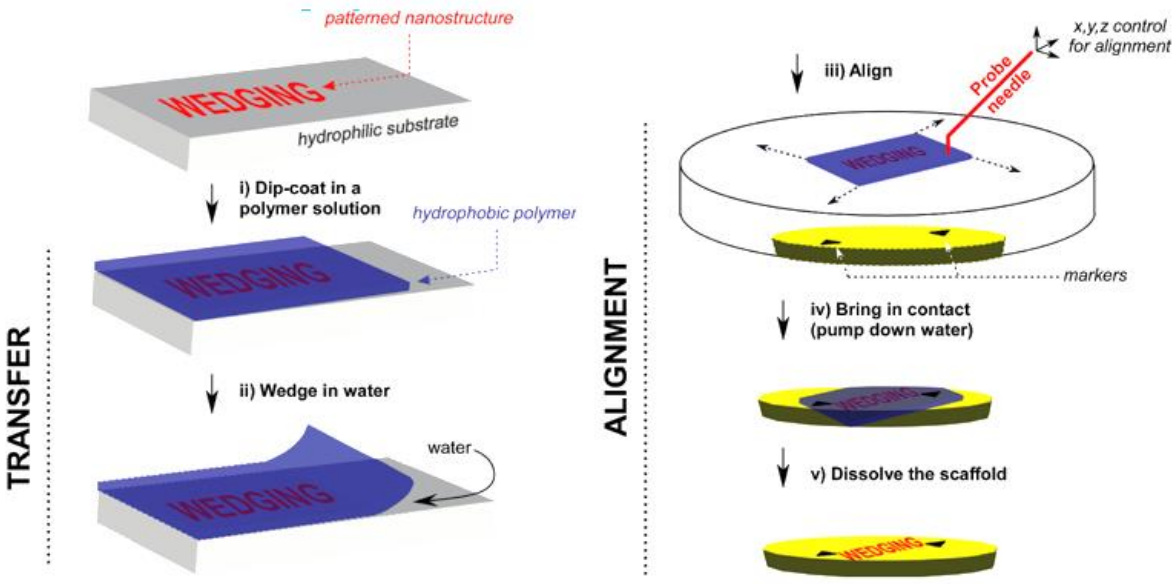

Annex I – WW transfer of 285 nm-thick graphene layers on a Si wafer produced by mechanical-exfoliation (a) on a target SiN membrane (b, dark-green square). Transfer was successful since (c) shows the graphene layer on top of the SiN membrane. Subsequent polymer dissolution in (d) leaves only the graphene layers on the SiN membrane. Scale bar is set to 10 μm.[43]

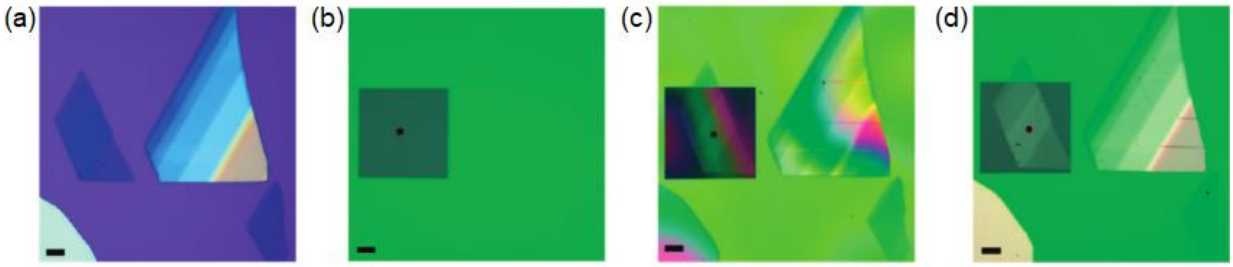

Annex J – Relation between transferred NW's length and AR length. Scale bar is set to 10 μm.[44]

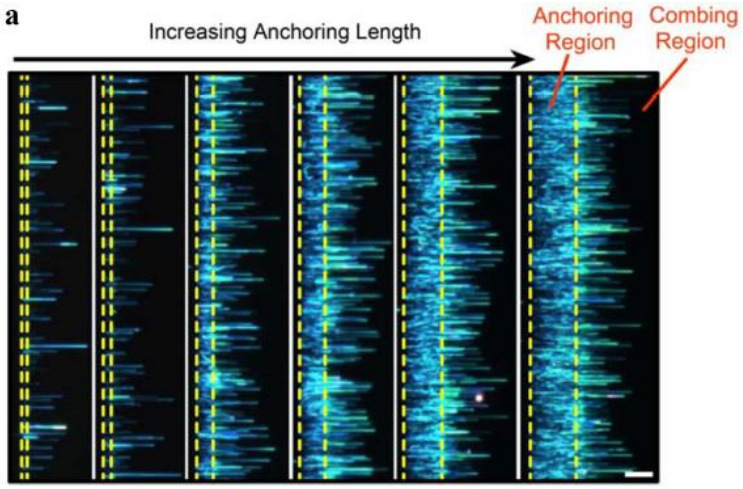

Annex K – Relation between AR's length (a) and CR layer thickness (b) with transferred NWD.[44]

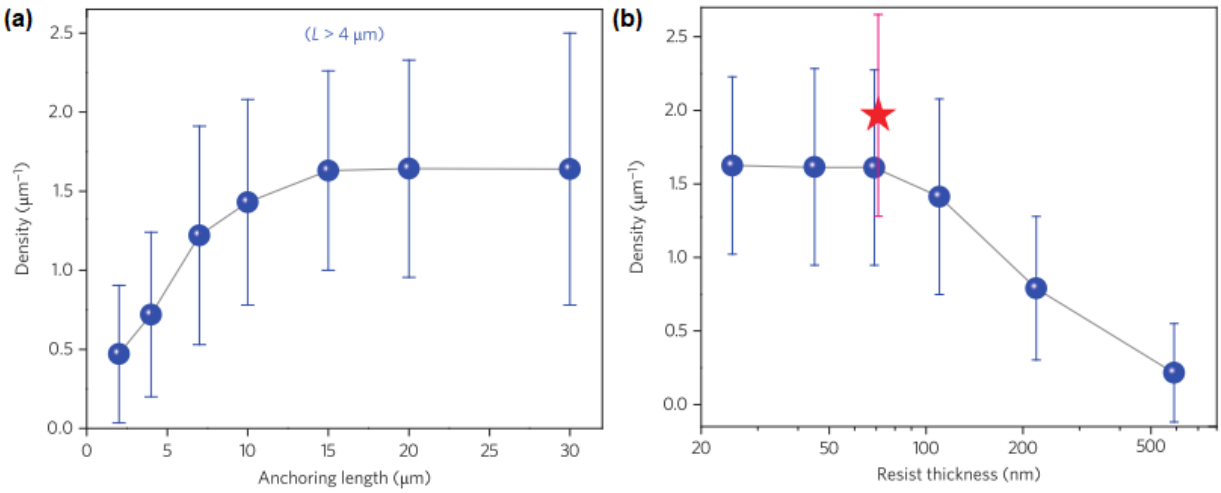

Annex L – Relation between transfer speed (a) and applied pressure (b) with transferred NWD.[44]

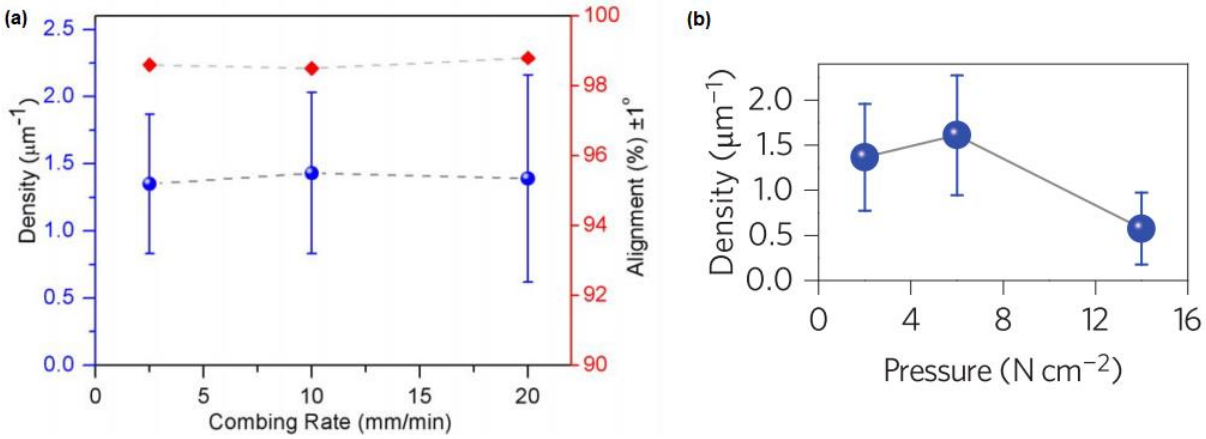

Annex M – NW transfer to a 3x11 mm^2 area (a) patterned with alternating 15x80 μm^2 sections (b) . Scale bar is set to (a) 100 μm and (b) 2 μm.[44]

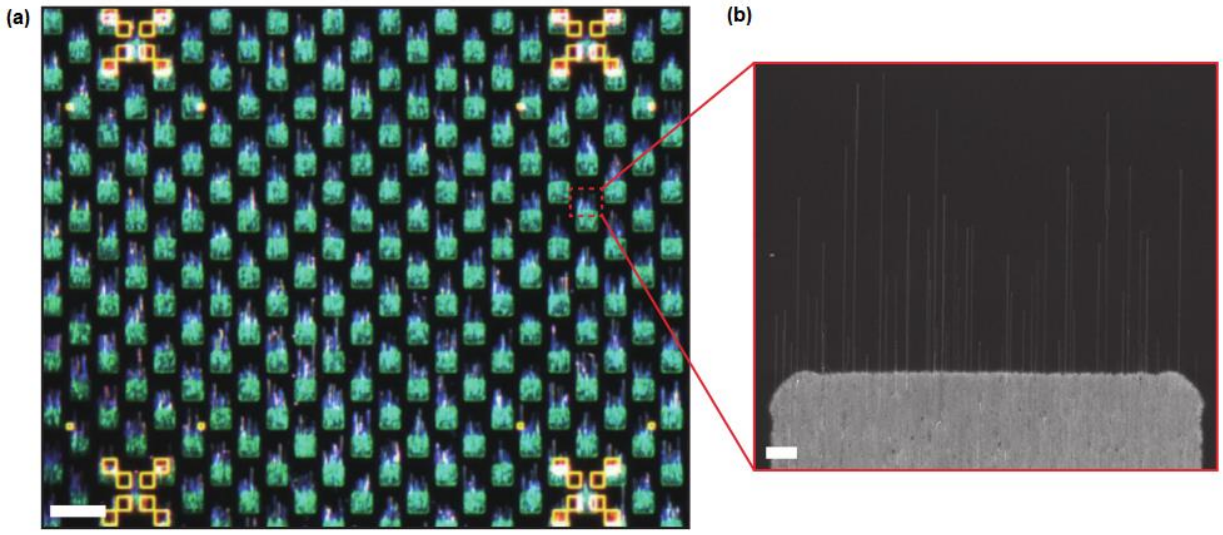

Annex N – Transferred 140 μm-long NWs with a 96% alignment within a variation of ± 1º.[44]

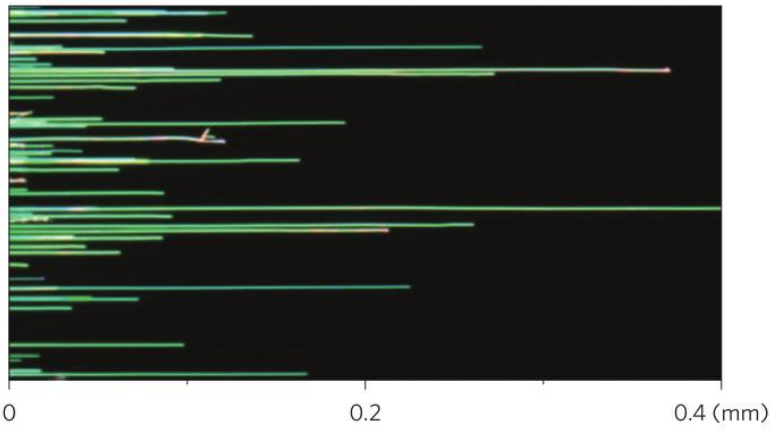

ANNEX O – CA measurements. Water drops were deposited in several areas.

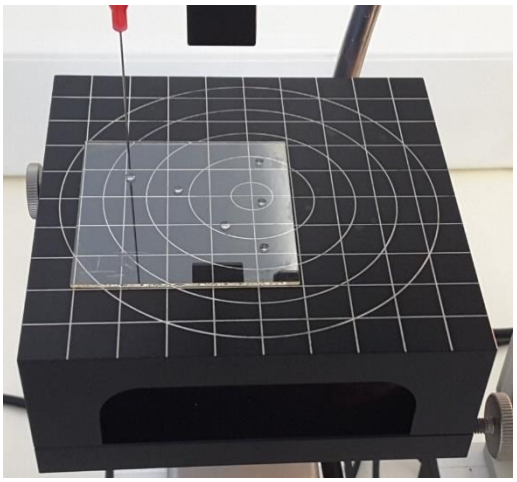

ANNEX P – PDMS rubbing motion on the NWs where (a) is with circular motion and (b) with unidirectional motion.

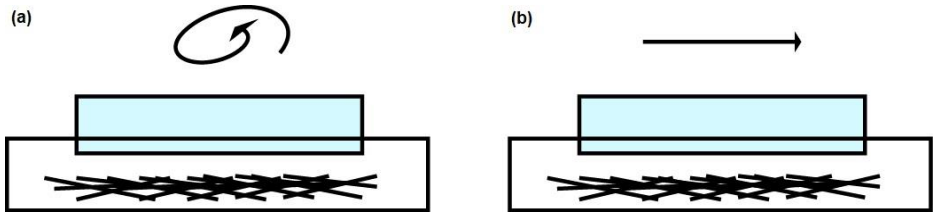

ANNEX Q – PDMS patterning initial designs.

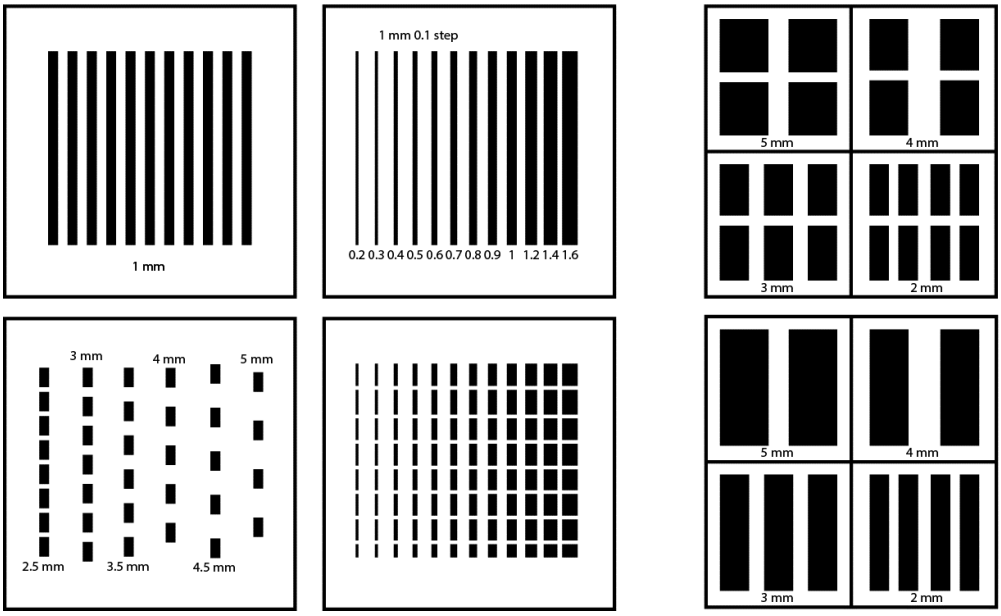

ANNEX R – Laser horizontal engraving scanning motion.

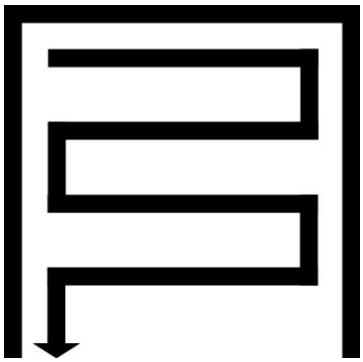

ANNEX S – Acrylic masters design upgrade. Pattern tracks are represented as the outside black lines, whether the engraving motion through the inner arrow.